Supporting information

Effect of chiral purity on adjuvanticity of archaeol-based glycolipids

Sophie Régnier[a], Edmond Lam[a], Vinicio Vasquez[a], Camilo F. Martinez-Farina[b], , Felicity C. Stark[c], Gerard Agbayani[c], Lise Deschatelets[c], Renu Dudani[c], Blair A. Harrison[c], Bassel Akache[c], Michael J. McCluskie[c*], and Usha D. Hemraz[a*]

[a]Aquatic and Crop Resource Development, National Research Council of Canada, 6100 Royalmount Avenue, Montreal, Quebec, H4P 2R2, Canada

[b]Aquatic and Crop Resource Development Research Center, National Research Council of Canada, Halifax, Nova Scotia, B3H 3Z1, Canada

[c]Human Health Therapeutics, National Research Council of Canada, 1200 Montreal Rd, Ottawa, Ontario, K1A 0R6, Canada

Table of Contents

1. Optical rotation

For comparative purposes, optical rotations were measured on a Rudolph Autopol I polarimeter for samples prepared in chloroform. The specific rotation $[\alpha]_D^T$ values (Table S1) for archaeol and sucrose samples were obtained using a 100 mm polarimeter cell; D refers to the D-line of sodium (589 nm); Temperatures (T) are given in degrees Celsius (°C). Control and calibration experiments were also conducted using sucrose (Caledon, catalog # 8720-1, lot# 83129).

Table S1. Specific rotation of archaeols and sucrose

Sample	Concentration (g/100 mL)	Specific rotation ($°dm^{-1}cm^3g^{-1}$)	Temp. (°C)
Archaeol **1**	4.96	9.68	24.6
Archaeol **2**	1.92	9.38	25.0
Archaeol **3**	0.84	0	25.0
Sucrose	20.02	66.28	25.6
Sucrose	10.01	68.33	25.5
Sucrose	5.01	67.66	25.2
Sucrose	1.00	69.00	25.2
Sucrose	0.50	70.00	25.1

2. Synthesis and characterization

SLA-1 and SLA-2 was synthesized according to a previously reported procedure that employs the bacterial archaeol *1*.[1-2]

Compound SLA-1. ^{1}HNMR (1:1 CD_3OD/CD_2Cl_2, 700 MHz) δ 4.32 (dd, 2H, *J1* = 2.8 Hz, *J2* = 7.7 Hz), 4.28 (brt, 1H, *J1* = 9.5 Hz, *J2* = 10.9 Hz), 4.09 (dd, 1H, *J1* = 3.5 Hz, *J2* = 10.5 Hz), 3.93 (dd, 1H, *J1* = 3.5 Hz, *J2* = 10.5 Hz), 3.87-3.81 (m, 4H), 3.56-3.60 (m, 8H), 3.41 (tt, 1H, *J1* = 3.5 Hz, *J2* = 9.1 Hz), 3.30 (m, 1H), 1.39-1.05 (m, 44H), 0.89-0.84 (m, 30H); ^{13}CNMR (1:1 CD_3OD/CD_2Cl_2, 176 MHz) δ 105.0, 103.6, 83.0, 78.5, 75.5, 75.1, 74.3, 74.1, 73.7, 71.7, 70.7, 70.6, 69.7, 69.2, 69.2, 67.6, 62.0, 40.0, 38.1, 38.1, 38.0, 38.0, 38.0, 38.0, 38.0, 37.9, 37.6, 37.3, 33.5, 33.5, 33.4, 30.5, 30.5, 28.6, 25.4, 25.1, 25.0, 22.9, 22.8, 20.1, 20.0, 20.0, 20.0 ppm; HRMS (ESI-) calcd. for $C_{55}H_{108}O_{16}S$ $[M\text{-}Na+H]^-$: 1055.7285, found 1055.7276. $[\alpha]_D^{23}$ = -1.8° (c = 1.11, 1:1 CH_2Cl_2/MeOH). Anal. Calcd. For $C_{55}H_{107}NaO_{16}S$ (1078.72): C, 61.20; H, 9.99; N, 0.00, found C, 60.51; H, 9.83; N, 0.00.

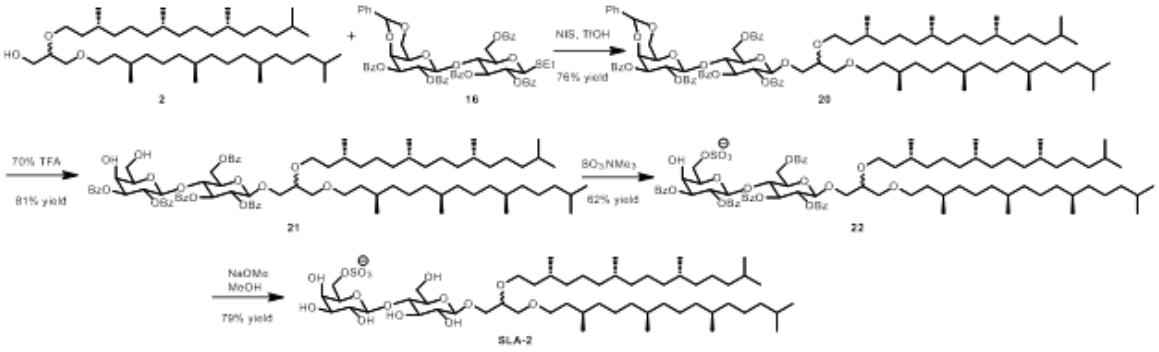

Scheme S1: Synthesis of SLA-2

Compound 20. ^{1}HNMR ($CDCl_3$, 700 MHz) δ 7.99 (d, 2H, *J* = 9.8 Hz), 7.94-7.87 (m, 8H), 7.57 (t, 1H, *J* = 10.5 Hz), 7.50-7.41 (m, 5H), 7.37-7.28 (m, 12H), 7.16 (t, 2H, *J* = 11.2 Hz), 5.84 (t, 1H, *J* = 12.6 Hz), 5.78 (dd, 1H, *J1* = 11.2 Hz, *J2* = 14.7 Hz), 5.34 (dd, 1H, *J1* = 10.5 Hz, *J2* = 13.3 Hz), 5.28 (s, 1H), 5.15 (dd, 1H, *J1* = 4.9 Hz, *J2* = 14.7 Hz), 4.83 (d, 1H, *J* = 11.2 Hz), 4.75 (d, 1H, *J* = 11.2 Hz), 4.61 (dd, 1H, *J1* = 2.8 Hz, *J2* = 16.8 Hz), 4.37 (dd, 1H, *J1* = 6.3 Hz, *J2* = 16.8 Hz), 4.30 (d, 1H, *J* = 4.9 Hz), 4.22 (t, 1H, *J* = 13.3 Hz), 3.86-3.83 (m, 2H), 3.77 (d, 1H, *J* = 16.1 Hz), 3.57 (d, 1H, *J* = 14.7 Hz), 3.51-3.44 (m, 2H), 3.35-

3.21 (m, 6H), 2.95 (s, 1H), 1.40-1.56 (m, 4H), 1.25-1.00 (m, 44H), 0.88-0.81 (m, 24H), 0.77 (d, 3H, *J* = 6.5 Hz), 0.68 (d, 3H, *J* = 6.5 Hz); ^{13}CNMR ($CDCl_3$, 176 MHz) δ 166.3, 165.8, 165.4, 165.2, 165.0, 137.6, 133.5, 133.3, 133.2, 133.1, 130.0, 130.0, 129.8, 129.8, 129.7, 129.5, 129.0, 128.9, 128.5, 128.5, 128.4, 128.4, 128.4, 128.1, 126.5, 101.6, 101.1, 100.7, 77.8, 77.3, 77.2, 77.0, 76.9, 74.2, 73.2, 72.8, 72.7, 72.4, 70.7, 70.6, 70.1, 69.5, 69.2, 68.1, 66.5, 62.5, 39.5, 37.7, 37.6, 37.6, 37.6, 37.5, 37.4, 37.4, 37.0, 36.6, 33.0, 32.9, 30.0, 29.8, 28.1, 24.9, 24.6, 24.6, 24.5, 24.4, 22.9, 22.8, 19.9, 19.8, 19.6 ppm; HRMS (ESI+) calcd. for $C_{97}H_{132}O_{18}Na$ $[M+Na]^+$: 1607.9306, found 1607.9445.

Compound 21. ^{1}HNMR ($CDCl_3$, 700 MHz) δ 8.04 (d, 2H, *J* = 7.7 Hz), δ 7.97 (d, 2H, *J* = 7.7 Hz), δ 7.93 (d, 4H, *J* = 7.7 Hz), δ 7.91 (d, 2H, *J* = 7.7 Hz), 7.60 (t, 1H, *J* = 7.7 Hz), 7.56 (t, 1H, *J* = 10.5 Hz), 7.50-7.41 (m, 6H), 7.37-32 (m, 5H), 7.24 (t, 2H, *J* = 7.7 Hz), 5.44 (t, 1H, *J* = 7.7 Hz), 5.06 (dd, 1H, *J1* = 3.5 Hz, *J2* = 10.5 Hz), 4.76 (t, 2H, *J* = 7.7 Hz), 4.59 (dd, 1H, *J1* = 1.4 Hz, *J2* = 11.9 Hz), 4.42 (dd, 1H, *J1* = 4.2 Hz, *J2* = 11.9 Hz), 4.19-4.17 (m, 2H), 3.88 (dd, 1H, *J1* = 2.8 Hz, *J2* = 10.5 Hz), 3.83 (m, 1H), 3.51-3.47 (m, 2H), 3.37-3.32 (m, 4H), 3.28-3.24 (m, 5H), 1.55-0.95 (m, 48H), 0.89-0.81 (m, 24H), 0.77 (d, 3H, *J* = 5 Hz), 0.68 (d, 3H, *J* = 4.5 Hz); ^{13}CNMR (1:1 CD_3OD/CD_2Cl_2, 176 MHz) δ 66.0, 165.9, 165.5, 165.3, 165.2, 133.7, 133.5, 133.4, 133.4, 133.3, 130.0, 130.0, 129.9, 129.9, 129.8, 129.8, 129.7, 129.6, 129.3, 129.0, 128.8, 128.6, 128.5, 128.5, 101.4, 101.2, 74.3, 74.1, 73.7, 72.9, 71.9, 70.7, 70.6, 70.1, 69.7, 69.3, 68.4, 62.7, 62.7, 39.5, 37.6, 37.6, 37.5, 37.5, 37.4, 37.4, 37.0, 36.6, 32.9, 32.9, 32.9, 30.0, 29.7, 28.1, 24.9, 24.6, 24.6, 24.5, 24.4, 22.9, 22.8, 22.8, 21.2, 19.9, 19.8, 19.8, 19.6 ppm; HRMS (ESI+) calcd, for $C_{90}H_{128}O_{18}Na$ $[M+Na]^+$: 1519.8993, found 1519.8977.

Compound 22. ^{1}HNMR (1:1 CD_3OD/CD_2Cl_2, 700 MHz) δ 8.00 (d, 2H, *J* = 7.7 Hz), 7.94-7.91 (m, 6H), 8.00 (d, 2H, *J* = 7.7 Hz), 7.86 (d, 2H, *J* = 7.7 Hz), 7.55 (t, 1H, *J* = 7.7 Hz), 7.52 (t, 1H, *J* = 7.7 Hz), 7.49-7.43 (m, 5H), 7.38 (t, 2H, *J* = 7.7 Hz), 7.32 (t, 3H, *J* = 7.7 Hz), 7.23 (t, 2H, *J* = 7.7 Hz), 5.71 (t, 1H, *J* = 9.1 Hz), 5.62 (dd, 1H, *J1* = 7.7 Hz, *J2* = 9.8 Hz), 5.32 (m, 1H), 5.12 (dd, 1H, *J1* = 3.5 Hz, *J2* = 10.5 Hz), 4.82 (d, 1H, *J* = 7.7 Hz), 4.74 (d, 1H, *J* = 7.7 Hz), 4.58 (dd, 1H, *J1* = 1.4 Hz, *J2* = 11.9 Hz), 4.41 (dd, 1H, *J1* = 4.9 Hz, *J2* = 11.9 Hz), 4.21 (t, 1H, *J* = 9.1 Hz), 4.15 (d, 1H, *J* = 2.8 Hz), 3.83 (m, 2H), 3.57 (d, 3H),

3.45 (m, 1H), 3.42 (m, 1H), 3.31 (m, 2H), 3.20 (m, 4H), 1.50 (m, 4H), 1.42-0.81 (m, 68H); 0.75 (d, 3H, *J* = 7.0 Hz), 0.68 (d, 3H, *J* = 6.3 Hz); ^{13}CNMR (1:1 CD_3OD/CD_2Cl_2, 176 MHz) δ 166.4, 166.4, 166.2, 165.9, 165.7, 134.0, 133.7, 133.7, 133.6, 130.0, 130.0, 129.9, 129.9, 129.9, 129.7, 129.6, 129.2, 128.9, 128.8, 128.8, 128.7, 101.8, 101.4, 77.9, 76.9, 74.4, 73.8, 73.3, 73.0, 72.5, 70.7, 70.6, 70.4, 70.2, 69.2, 65.8, 64.1, 62.9, 39.7, 37.8, 37.8, 37.8, 37.7, 37.7, 37.7, 37.7, 37.6, 37.6, 37.2, 36.8, 33.1, 30.2, 30.0, 28.3, 25.1, 24.8, 24.8, 24.7, 24.6, 19.8, 19.8, 19.7, 19.6 ppm HRMS (ESI-) calcd, for $C_{90}H_{128}O_{21}S$ $[M-Na+H]^-$: 1575.8596, found 1575.9055.

Compound SLA-2. ^{1}HNMR (1:1 CD_3OD/CD_2Cl_2, 700 MHz) δ 4.33 (brt, 2H, *J1* = 6.3 Hz, *J2* = 7.7 Hz), 4.27 (brt, 1H, *J1* = 9.1 Hz, *J2* = 10.5 Hz), 4.11 (dd, 1H, *J1* = 4.2 Hz, *J2* = 11.2 Hz), 3.93 (dd, 1H, *J1* = 4.2 Hz, *J2* = 10.5 Hz), 3.88-3.84 (m, 4H), 3.67-3.48 (m, 12H), 3.42-3.41 (m, 1H), 3.31-3.30 (m, 1H), 1.64-1.05 (m, 44H), 0.90-0.84 (m, 30H); ^{13}CNMR (1:1 CD_3OD/CD_2Cl_2, 175 MHz) δ 105.1, 103.8, 82.8, 78.8, 78.7, 75.7, 75.4, 74.4, 74.1, 73.9, 71.8, 71.1, 70.7, 70.7, 69.8, 69.8, 69.5, 69.4, 69.3, 67.7, 62.0, 40.2, 38.2, 38.2, 38.2, 38.2, 38.1, 38.1, 38.1, 38.0, 37.7, 37.4, 33.6, 33.6, 33.6, 30.6, 30.6, 28.8, 25.6, 25.2, 25.2, 25.2, 25.2, 25.2, 23.0, 22.9, 20.1, 20.1, 20.1, 20.1, 20.0, 19.9 ppm; HRMS (ESI-) calcd. for $C_{55}H_{108}O_{16}S$ $[M-Na+H]^-$: 1055.7285, found 1055.7282. $[\alpha]_D^{23}$ = -2.67° (c = 1.87, 1:1 $CHCl_3$/MeOH). Anal. Calcd. For $C_{55}H_{107}NaO_{16}S$ (1078.72): C, 61.20; H, 9.99; N, 0.00, found C, 60.67; H, 9.82; N, 0.00.

3. LC-HRMS analysis of archaeol

Prior to conducting the chiral HPLC analysis, HRMS was used to confirm the identity of the compounds. The latter were analyzed by infusion, in which the sample (e.g., archaeol at 10 µg/L in methanol) is infused into the mobile phase flow and passes directly into the mass spectrometer (TOF). Ammonium acetate (5 mM) and methanol were used as mobile phases at a flow of 0.1 mL/min. The compounds were identified using the exact mass of the molecular ion $[M+H]^+$ and the isotopic distribution. The mass spectrometer was set to full MS scan from 100 m/z to 1500 m/z and operated in positive ionization mode. Archaeol has a chemical formula of $C_{43}H_{88}O_3$ and exact mass of 652.6733; The $[M+H]^+$ ion has an exact mass of 653.6806.

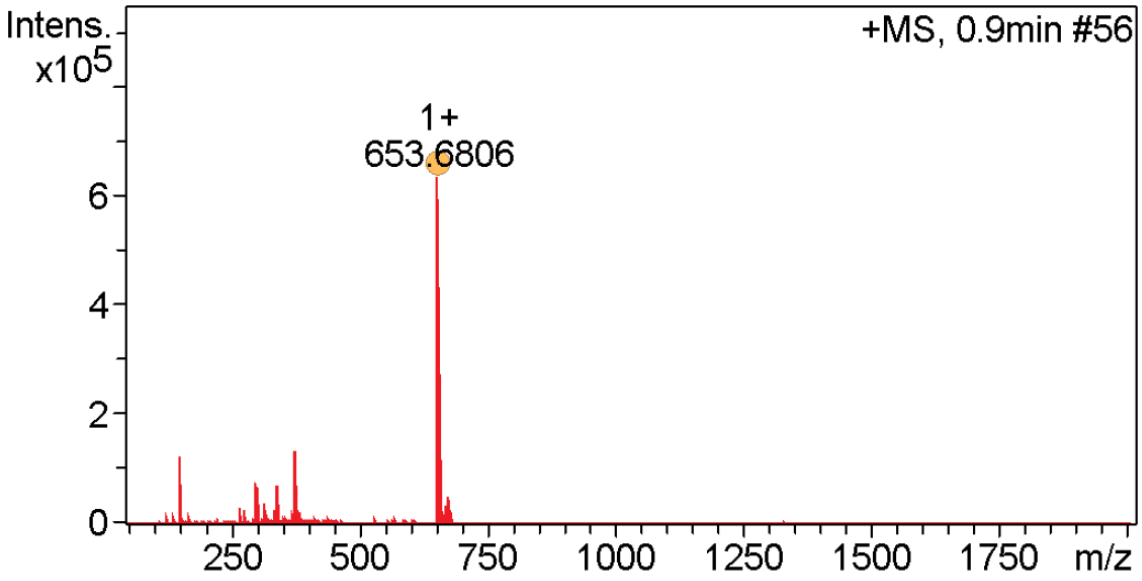

#	m/z	Res.	S/N	I	I %	FWHM
1	653.6806	9105	5171.4	634687	100.0	0.0718
2	654.6837	9348	2540.8	311469	49.1	0.0700
3	655.6859	9795	653.9	80137	12.6	0.0669
4	656.6888	10054	107.3	13148	2.1	0.0653

Figure S1. Mass spectrum of archaeol **1** (100% R) showing the $[M+H]^+$ ion at m/z 653.6806 and the expected isotopic ratio (theoretical pattern: 653.6806 (100.0%); 654.6840 (47.6%); 655.6873 (11.7%); 656.6905 (2.0%)).

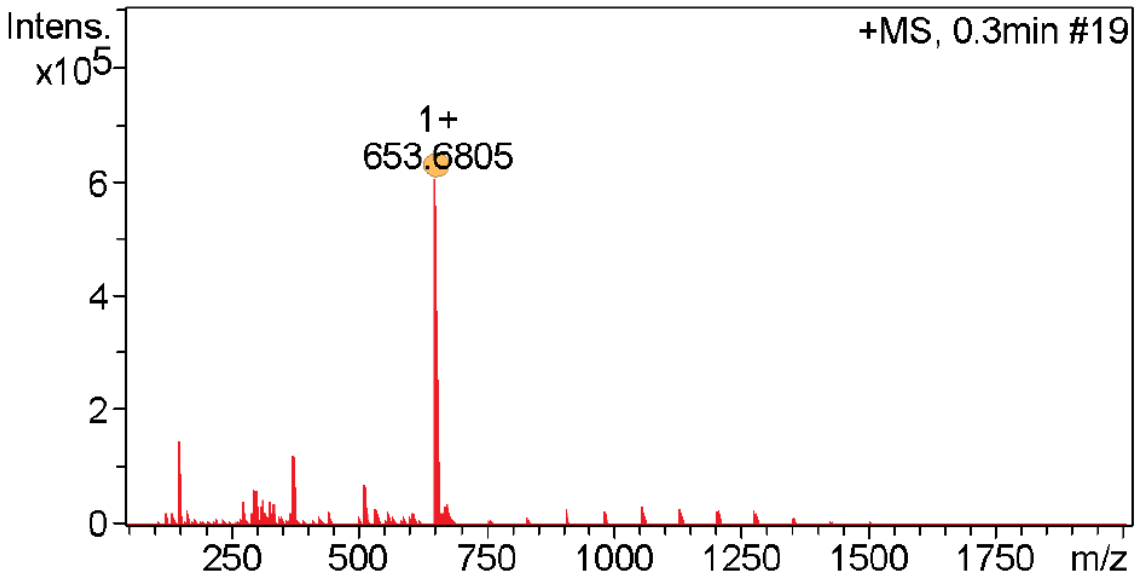

#	m/z	Res.	S/N	I	I %	FWHM
1	653.6805	9275	3808.2	605108	100.0	0.0705
2	654.6837	9512	1829.6	290699	48.0	0.0688
3	655.6855	9878	426.5	67763	11.2	0.0664
4	656.2196	7106	7.9	1252	0.2	0.0923
5	656.6892	9821	74.6	11858	2.0	0.0669
6	657.2215	8760	5.4	851	0.1	0.0750
7	657.6766	5605	10.2	1622	0.3	0.1173

Figure S2. Mass spectrum of archaeol **2** (94% R) showing the $[M+H]^+$ ion at m/z 653.6805 and the expected isotopic ratio (theoretical pattern: 653.6806 (100.0%); 654.6840 (47.6%); 655.6873 (11.7%); 656.6905 (2.0%)).

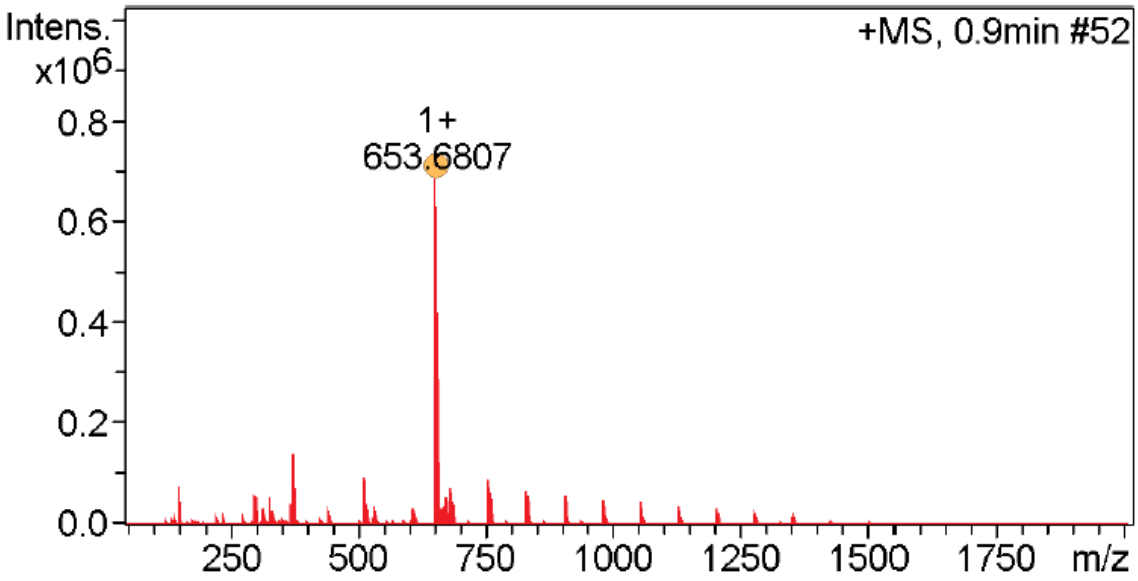

#	m/z	Res.	S/N	I	I %	FWHM
1	653.6807	9216	4190.8	684002	100.0	0.0709
2	654.2355	3377	16.3	2660	0.4	0.1937
3	654.6834	9459	2020.8	329820	48.2	0.0692
4	655.1680	3363	8.4	1377	0.2	0.1948
5	655.6859	9698	488.3	79701	11.7	0.0676
6	656.2209	8817	15.2	2487	0.4	0.0744
7	656.6875	9521	82.4	13441	2.0	0.0690
8	657.2297	10261	9.8	1599	0.2	0.0640
9	657.6929	9136	12.3	2000	0.3	0.0720

Figure S3. Mass spectrum of archaeol **3** (mixture of stereoisomers) showing the $[M+H]^+$ ion at m/z 653.6807 and the expected isotopic ratio (theoretical pattern: 653.6806 (100.0%); 654.6840 (47.6%); 655.6873 (11.7%); 656.6905 (2.0%)).

4. Archaeol C8 reverse-phase chromatography for identification confirmation

The compounds were also characterized by reverse-phase chromatography on a C8 column Halo C8 (50 x 3.0 mm, particle size 2.7 µm) from Advance Materials Technology) for identity confirmation. Ammonium acetate (5 mM) and methanol were used as mobile phases at a flow of 0.5 mL/min. A gradient of methanol from 95% to 100% within 2 min was used to elute the compound. The mass spectrometer (TOF) was set to full MS scan from 100 m/z to 1500 m/z and operated in positive ionization mode. The molecular ion $[M+H]^+$ at m/z 653.6806, the ammonium adduct $[M+NH_4]^+$ at m/z 670.7072, and a fragment at m/z 373.3676 corresponding to the loss of a phytyl unit, were monitored to confirm the identity of compound. The same retention times (4.3 min) were obtained for the molecular ion 653.6806 m/z, ammonium adduct 670.7072 m/z and fragment 373.3676 m/z for the three archaeol samples.

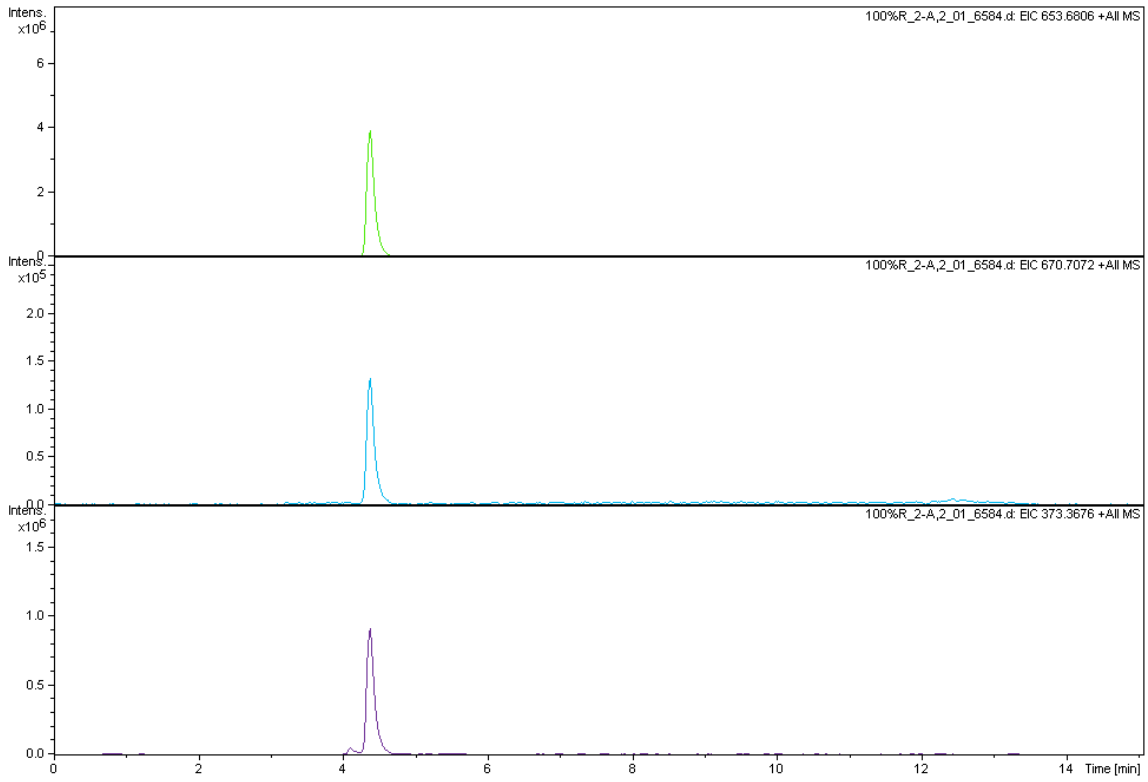

Figure S4. Extracted ion chromatograms (m/z 653.6806, 670.7072 and 373.3676) for archaeol **1** (100% R).

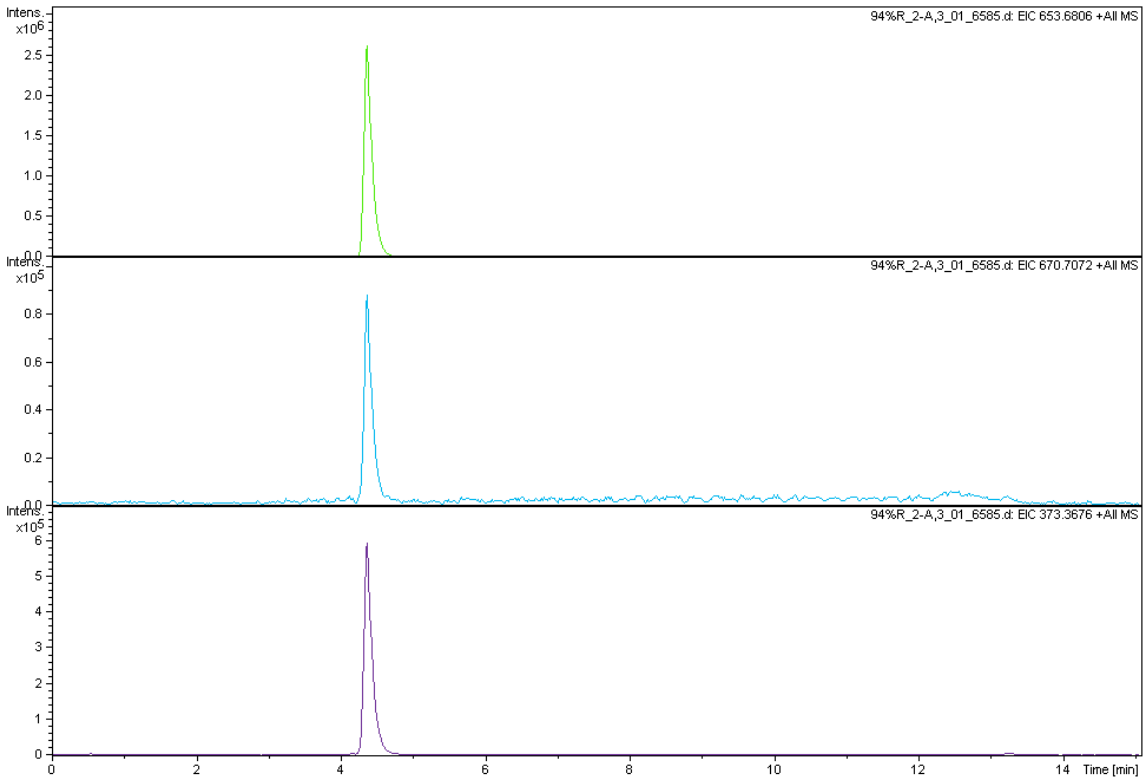

Figure S5. Extracted ion chromatograms (m/z 653.6806, 670.7072 and 373.3676) for archaeol **2** (94% R).

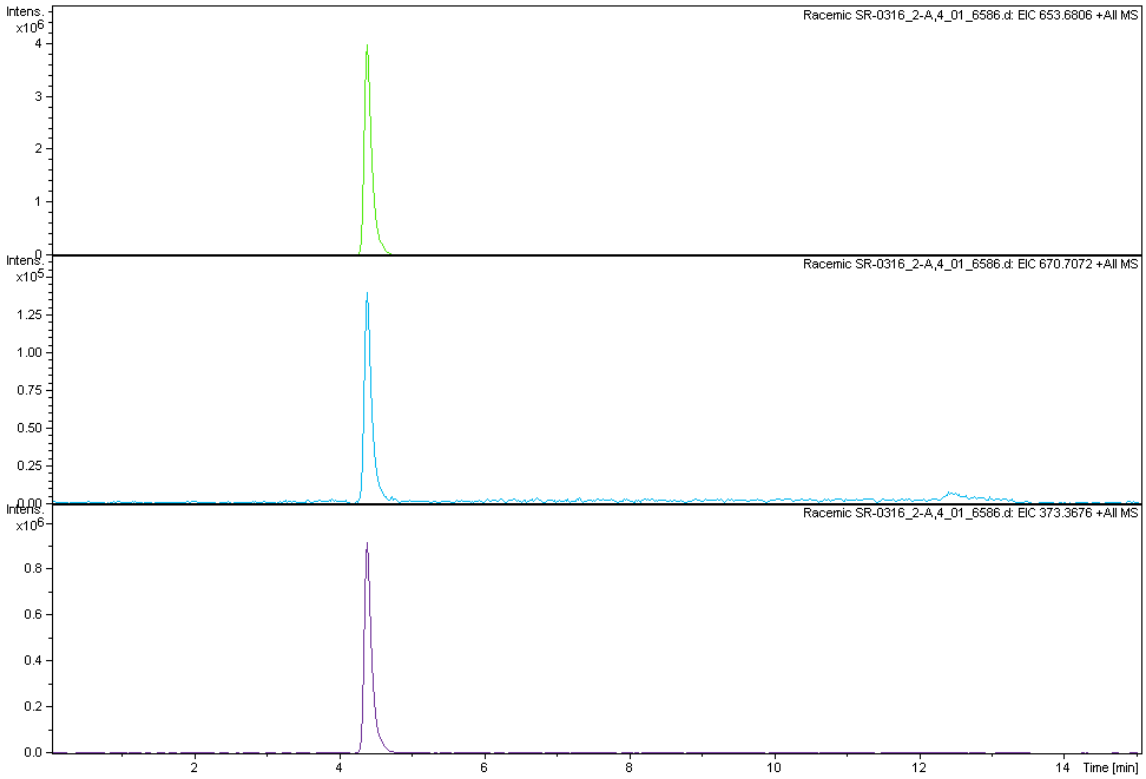

Figure S6. Extracted ion chromatograms (m/z 653.6806, 670.7072 and 373.37) for archaeol **3** (mixture of stereoisomers).

5. Chiral chromatography (polar organic) for elucidation of stereoisomers

The elucidation of the various stereoisomers in the archaeol samples was attempted on a Lux immobilized phase chiral column (amylose tris (3- chloro-5-methylphenylcarbamate), Lux i-Amylose-3 (250 x 4.6 mm, particle size 3 µm) from Phenomenex Inc.) Tests were performed in isocratic mobile phase conditions (not all conditions shown). A single quadrupole mass spectrometer was used for detection and was set to Selected Ion Mass (SIM) and operated in positive ionization mode. The molecular ion $[M+H]^+$ at m/z 653.65, the ammonium adduct $[M+NH_4]^+$ at m/z 670.65, and a fragment at m/z 373.35 corresponding to the loss of a phytyl unit, were monitored to confirm the identity of compound.

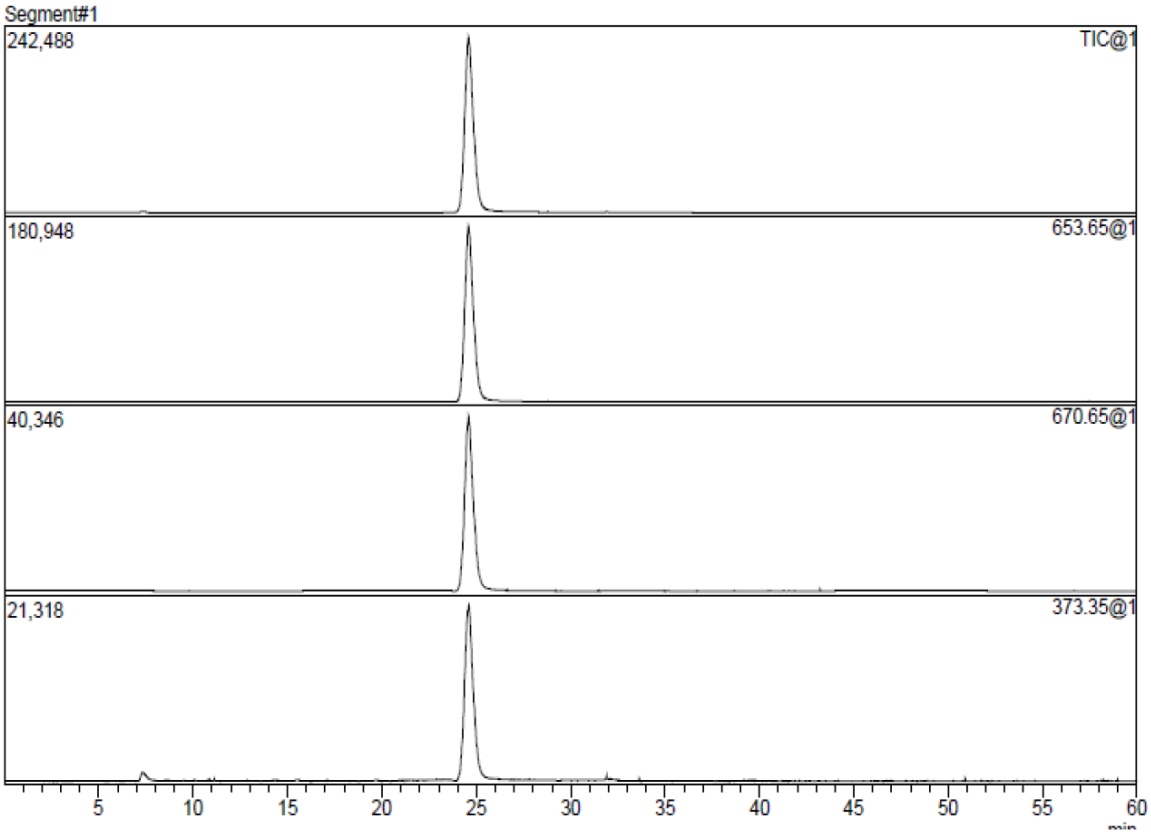

Figure S7. Total ion and extracted ion (m/z 653.65, 670.65 and 373.35) chromatograms for archaeol **1** (100% R) using chiral chromatography in polar organic mode. Methanol was used as mobile phases at a flow of 0.4 mL/min with a post-column addition of 5 mM ammonium acetate at a flow of 0.1 mL/min.

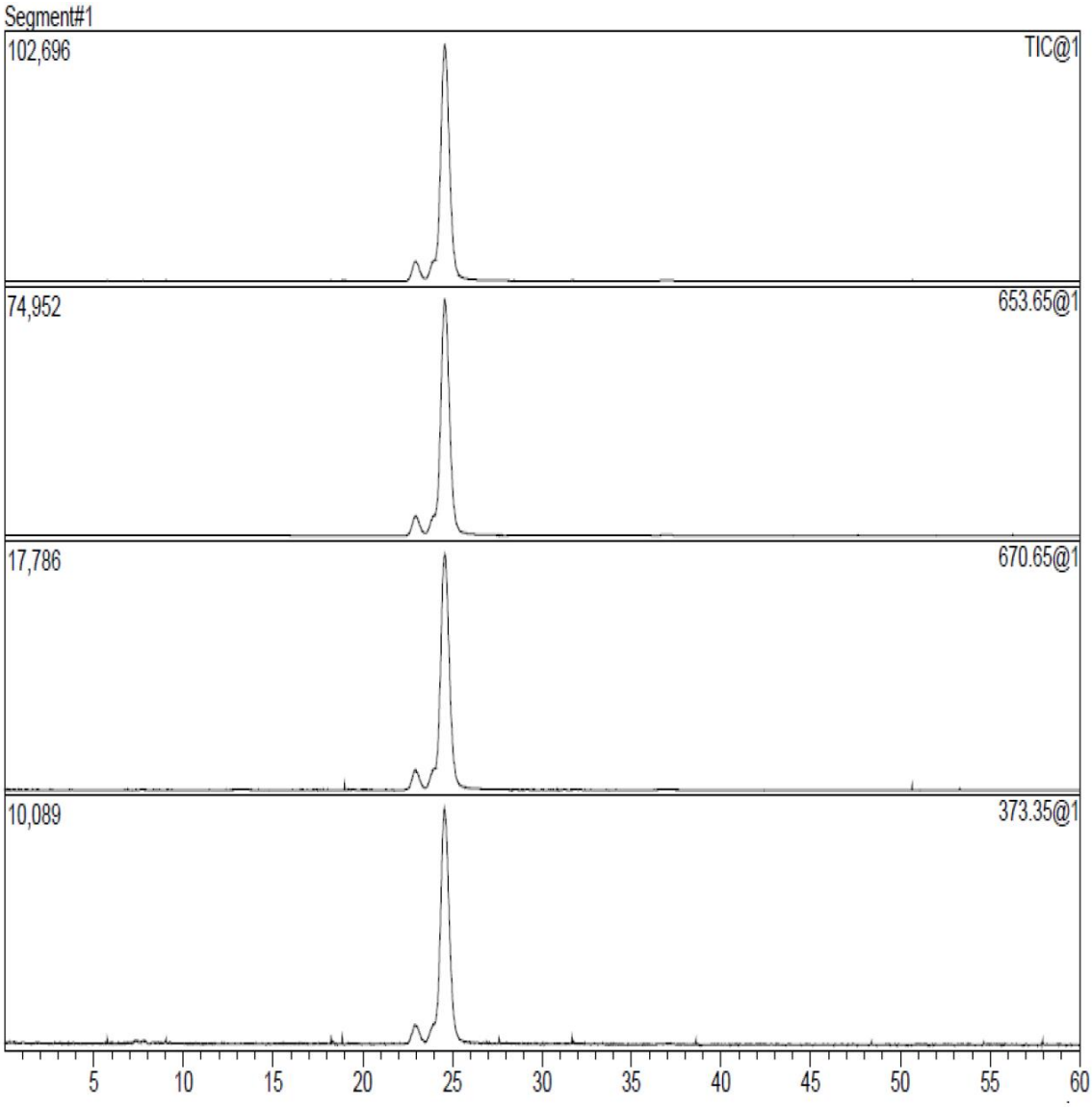

Figure S8. Total ion and extracted ion (m/z 653.65, 670.65 and 373.35) chromatograms for archaeol **2** (94% R) using chiral chromatography in polar organic mode. Methanol was used as mobile phases at a flow of 0.4 mL/min with a post-column addition of 5 mM ammonium acetate at a flow of 0.1 mL/min.

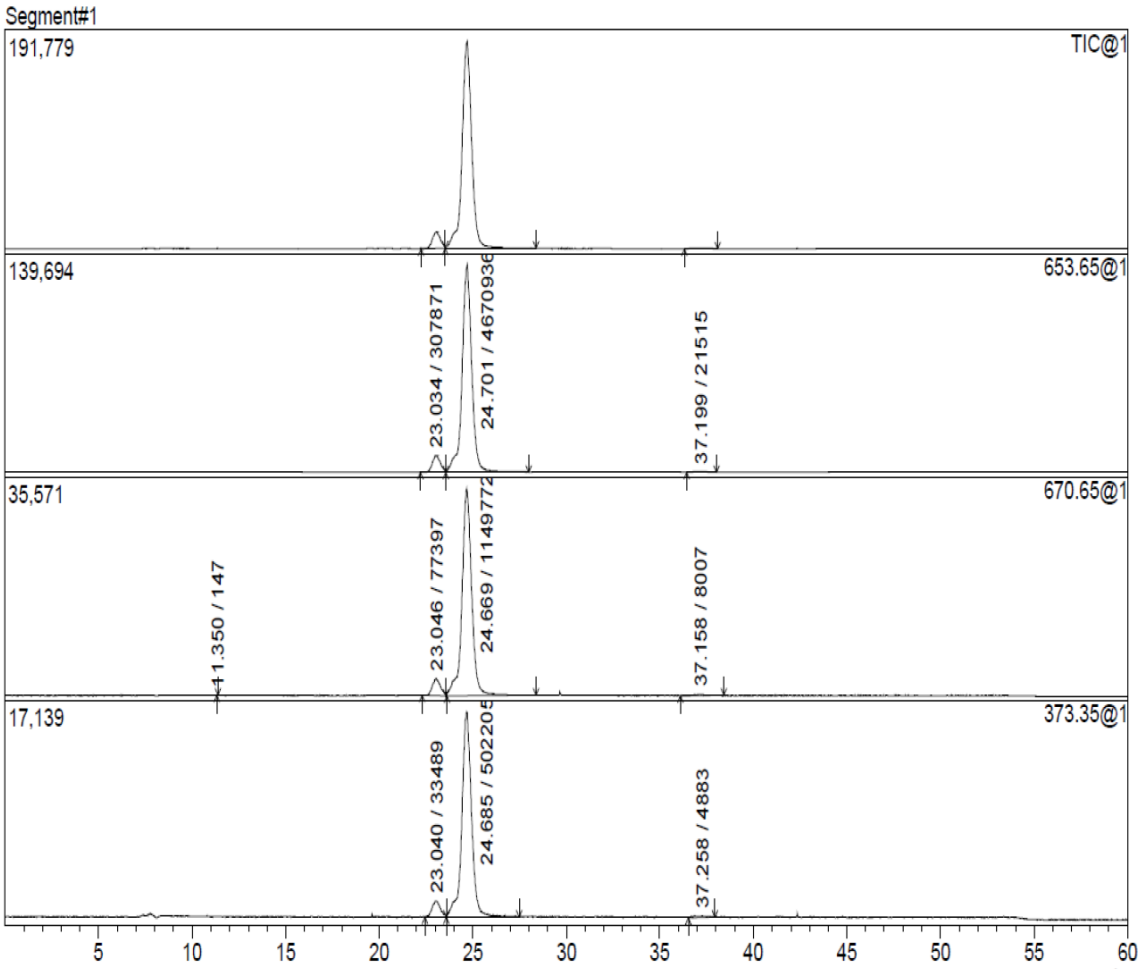

Ion m/z	Peak Area (S) RT: 23.0 min	Peak Area (R) RT: 24.7 min	Total Area	(%) R	(%) S
653.65	307871	4670936	4978807	93.82	6.18
760.65	77397	1149772	1227169	93.69	6.31
373.35	33489	502205	535694	93.75	6.25

Figure S9. HPLC chiral purity of R and S isomers of archaeol **2** using chiral chromatography in polar organic mode. Methanol was used as mobile phases at a flow of 0.4 mL/min with a post-column addition of 5 mM ammonium acetate at a flow of 0.1 mL/min.

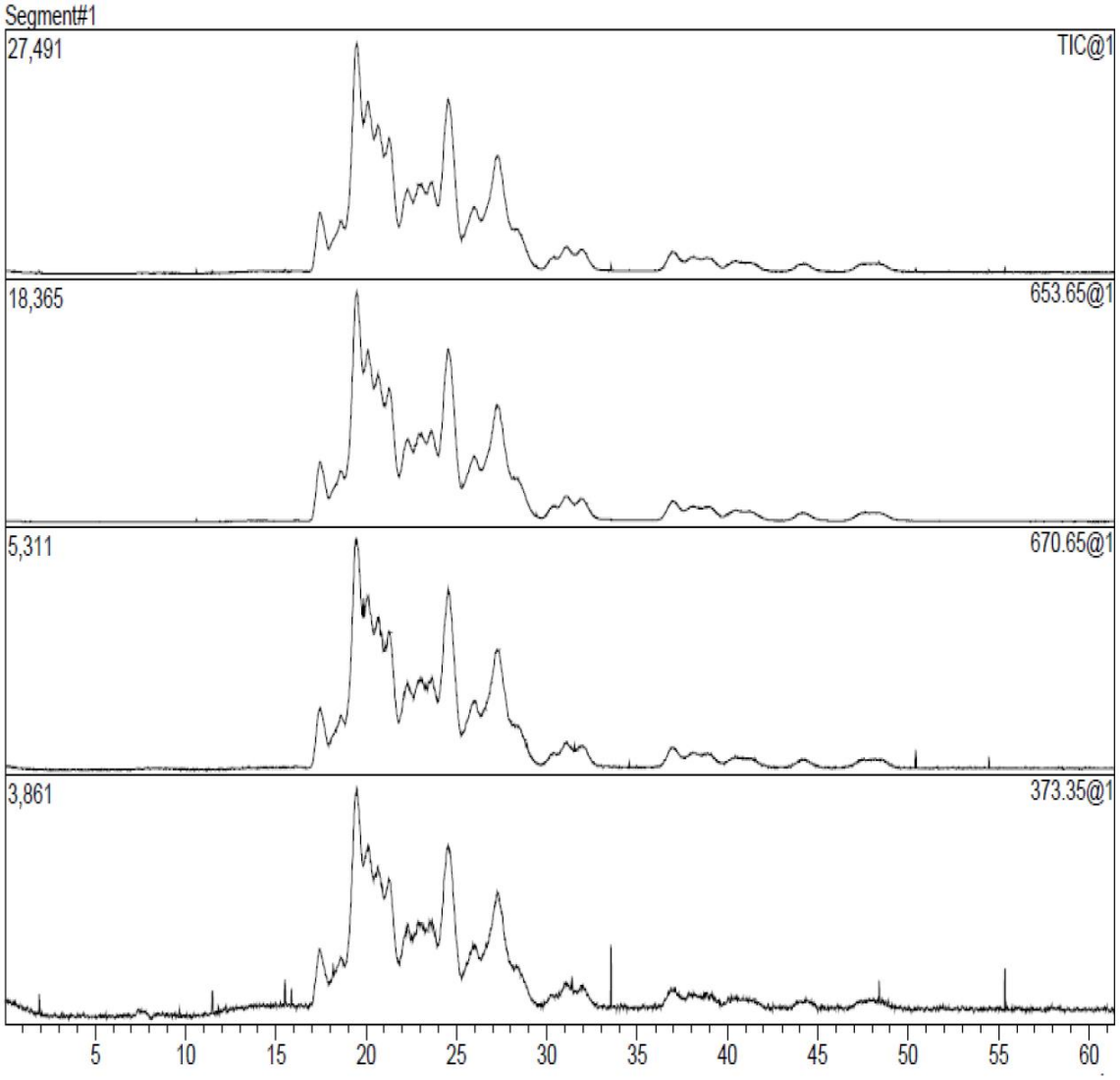

Figure S10. Total ion and extracted ion (m/z 653.65, 670.65 and 373.35) chromatograms for archaeol **3** (mixture of stereoisomers) using chiral chromatography in polar organic mode. Methanol was used as mobile phases at a flow of 0.4 mL/min with a post-column addition of 5 mM ammonium acetate at a flow of 0.1 mL/min.

6. LC-HRMS analysis of phytol

Given that the extracted ion chromatogram of archaeol **3** showed a highly complex chiral composition with more than 20 peaks showing the same molecular ion $[M+H]^+$ at m/z 653.65, the analysis of phytol **7** by HRMS was done. The latter was analyzed by infusion, in which the sample is infused into the mobile phase flow and passes directly into the mass spectrometer (TOF). Ammonium acetate (5 mM) and methanol were used as mobile phases at a flow of 0.1 mL/min. The mass spectrometer was set to full MS scan from 100 m/z to 1500 m/z and operated in positive ionization mode. Phytol has a chemical formula of $C_{20}H_{40}O$ and exact mass of 296.3079; The $[M+H]^+$ ion has an exact mass of 297.3152.

(a)

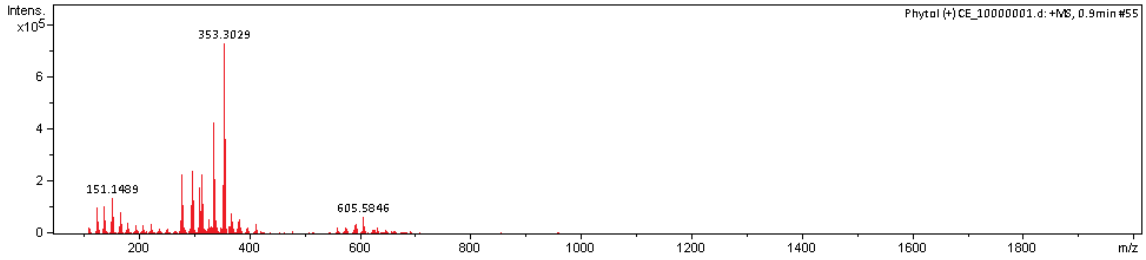

(b)

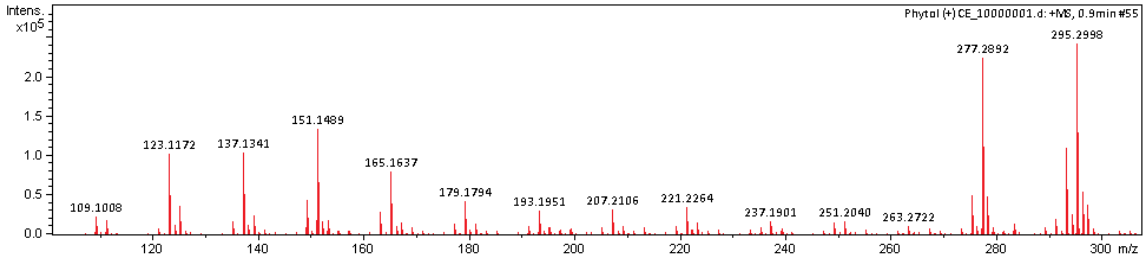

Figure S11. Mass spectrum of phytol **7** (97% mixture of isomers) showing the full spectrum (a) and a zoomed area between 100-300 m/z (b). The molecular ion $[M+H]^+$ ion at m/z 297.3152 has a low intensity and fragments are generated rapidly.

#	m/z	Res.	S/N	I	I %	FWHM
1	109.1008	4831	1116.6	21875	9.1	0.0226
2	111.1162	4699	898.3	17906	7.5	0.0236
3	123.1172	5165	4627.3	100774	41.9	0.0238
4	125.1324	5011	1634.1	35720	14.9	0.0250
5	135.1183	5237	714.1	17265	7.2	0.0258
6	137.1341	5277	4252.9	103294	43.0	0.0260
7	139.1470	5084	963.8	23485	9.8	0.0274
8	149.1334	5762	1702.2	44376	18.5	0.0259
9	151.1489	5502	5098.9	133324	55.5	0.0275
10	152.1522	5805	641.8	16859	7.0	0.0262
11	153.1609	5756	685.5	18026	7.5	0.0266
12	163.1479	6028	1040.5	29257	12.2	0.0271
13	165.1638	6091	2789.5	79544	33.1	0.0271
14	179.1792	5931	1241.8	41635	17.3	0.0302
15	193.1952	6306	801.4	30372	12.6	0.0306
16	207.2107	6562	731.3	31305	13.0	0.0316
17	221.2263	6649	733.8	34135	14.2	0.0333
18	223.1756	6192	307.4	14373	6.0	0.0360
19	237.1900	5894	332.6	16981	7.1	0.0402
20	249.2570	7105	278.4	14662	6.1	0.0351
21	251.2039	6797	315.0	16657	6.9	0.0370
22	275.2735	7151	858.3	49155	20.5	0.0385
23	277.2892	7345	3856.5	222413	92.6	0.0378
24	278.2926	7270	834.7	48215	20.1	0.0383
25	291.2751	5249	325.2	19515	8.1	0.0555
26	293.2843	7650	1815.7	110348	45.9	0.0383
27	294.2938	5681	424.2	25817	10.7	0.0518
28	295.2999	7242	3948.3	240264	100.0	0.0408
29	296.3054	6685	880.4	53533	22.3	0.0443
30	297.3130	6980	597.4	36478	15.2	0.0426

Figure S12. Phytol **7** (97% mixture of isomers) showing the 30 most abundant peaks within the mass spectrum between 100-300 m/z. The molecular ion $[M+H]^+$ ion at m/z 297.3152 has a low intensity and fragments are generated rapidly. Most of the fragments reported by NIST and NIH can been seen; m/z 111, 123, 137, 151, 165, 179, 223, 249, 278, 295, and 296.

7. Phytol C8 reverse-phase chromatography for identification confirmation

Phytol **7** (97% mixture of isomers) was also characterized by reverse-phase chromatography on a C8 column for identity confirmation. Ammonium acetate (5 mM) and methanol were used as mobile phases at a flow of 0.5 mL/min. A gradient of methanol from 80% to 100% within 10 min was used to achieve peak separation and elute the compound. The DA detector was set from 190-950 nm and 210 nm was selected to monitored and confirm the identity of the compound.[3] The mass spectrometer (TOF) was set to full MS scan from 100 m/z to 1500 m/z and operated in positive ionization mode. The molecular ion $[M+H]^+$ at m/z 297.3152, reported fragments 295, 278, 165, 151, 123 and 111 were also monitored to confirm the identity of compound.[4] The same retention times (6.4 min) were obtained for the UV chromatogram, molecular ion and selected fragments.

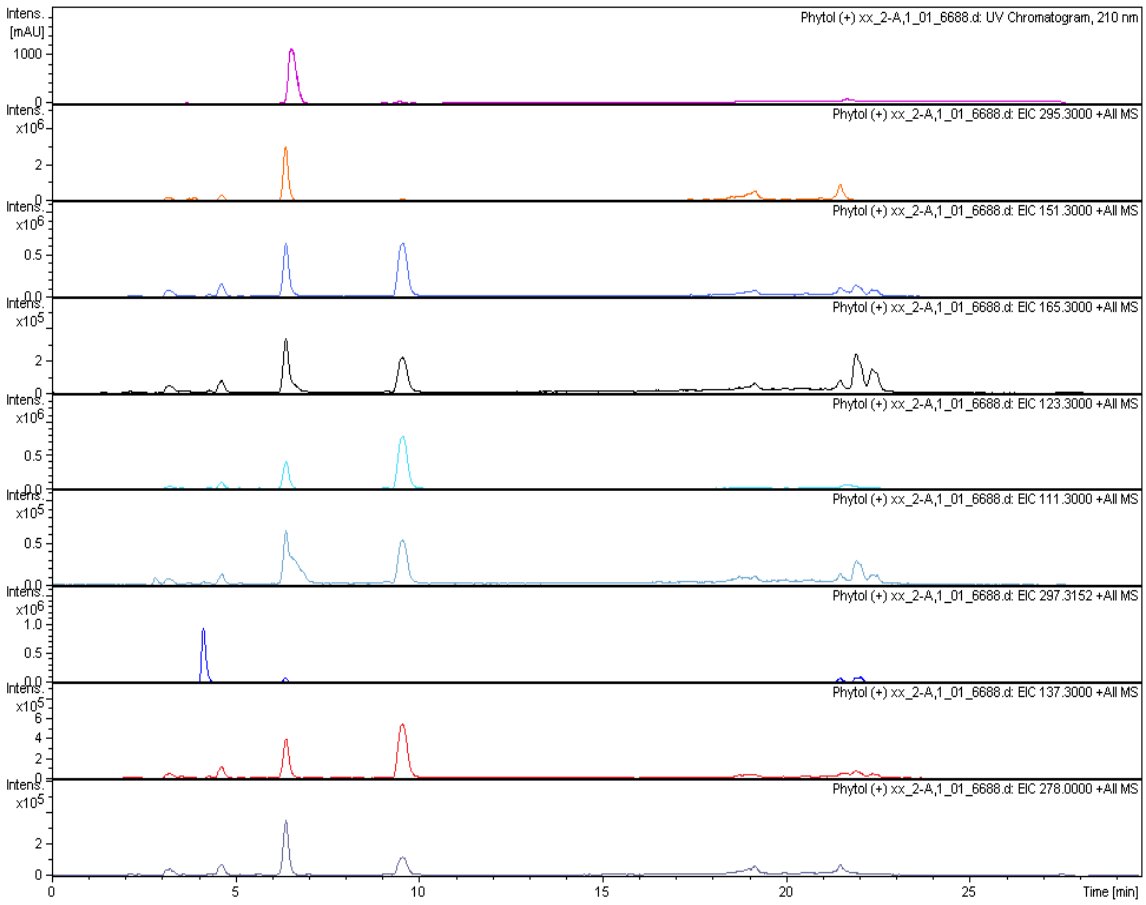

Figure S13. UV chromatogram and extracted ion chromatograms (m/z 297.3152 and fragments 295, 278, 165, 151, 137, 123 and 111) for phytol **7**.

8. Chiral chromatography (reverse phase) for elucidation of stereoisomers

The elucidation of the various stereoisomers in the archaeol samples was attempted on a Lux immobilized phase chiral column (amylose tris (3- chloro-5-methylphenylcarbamate)). Phytol **7** (97% mixture of isomers) was also analyzed and the molecular ion $[M+H]^+$ at m/z 297.3152, reported fragments 295, 278, 165, 151, 123 and 111, were also monitored. Tests were performed in isocratic mobile phase conditions (not all conditions shown). A single quadrupole mass spectrometer was used for detection and was set to selected ion mass (SIM) and operated in positive ionization mode. The molecular ion $[M+H]^+$ at m/z 653.65, the ammonium adduct $[M+NH_4]^+$ at m/z 670.65, and a fragment at m/z 373.35 corresponding to the loss of a phytyl unit, were monitored to confirm the identity of archaeol samples. Better resolution was obtained than the polar organic chromatography showing the shouldering minor peak of the R isomer (Figure S16). This confirms that within the 94% of (*R*)-2,3-bis(((3*R*,7*R*,11*R*)-3,7,11,15-tetramethylhexadecyl)oxy) propan-1-ol, there is a 6% of a different configuration of the chiral centers located on the phytanyl portion of the molecule, most probably at C3 of the phytyl unit. Again, as seen for the polar organic chromatography, a highly complex chiral composition can be noticed with more than 20 peaks showing the same molecular ion $[M+H]^+$ at m/z 653.65 but with better peak separation. The optically inactive archaeol **3**, with its 7 chiral centers, could have up to 128 enantiomer configurations ($2^7 = 128$), which explains the numerous peaks observed (Figure S17). The chromatograms for phytol **7** show more than 15 peaks with the same molecular ion $[M+H]^+$ at m/z 297.3 and reported fragments (Figure S18). This correlates with the highly complex chiral composition observed in the chiral chromatography of optically inactive archaeol **3** (Figure S17).

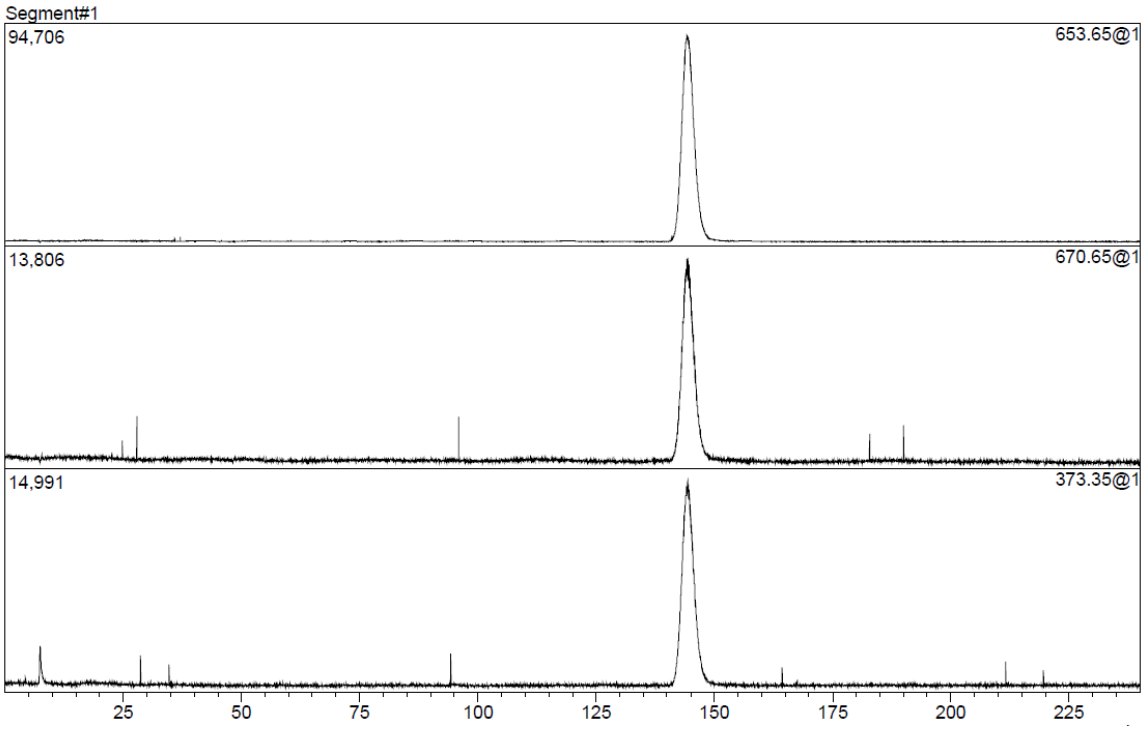

Figure S14. Total ion and extracted ion (m/z 653.65, 670.65 and 373.35) chromatograms for archaeol **1** (100% R) using chiral chromatography in polar organic mode. Methanol:H_2O 95:5% v/v was used as mobile phases at a flow of 0.4 mL/min with a post-column addition of 5 mM ammonium acetate at a flow of 0.1 mL/min.

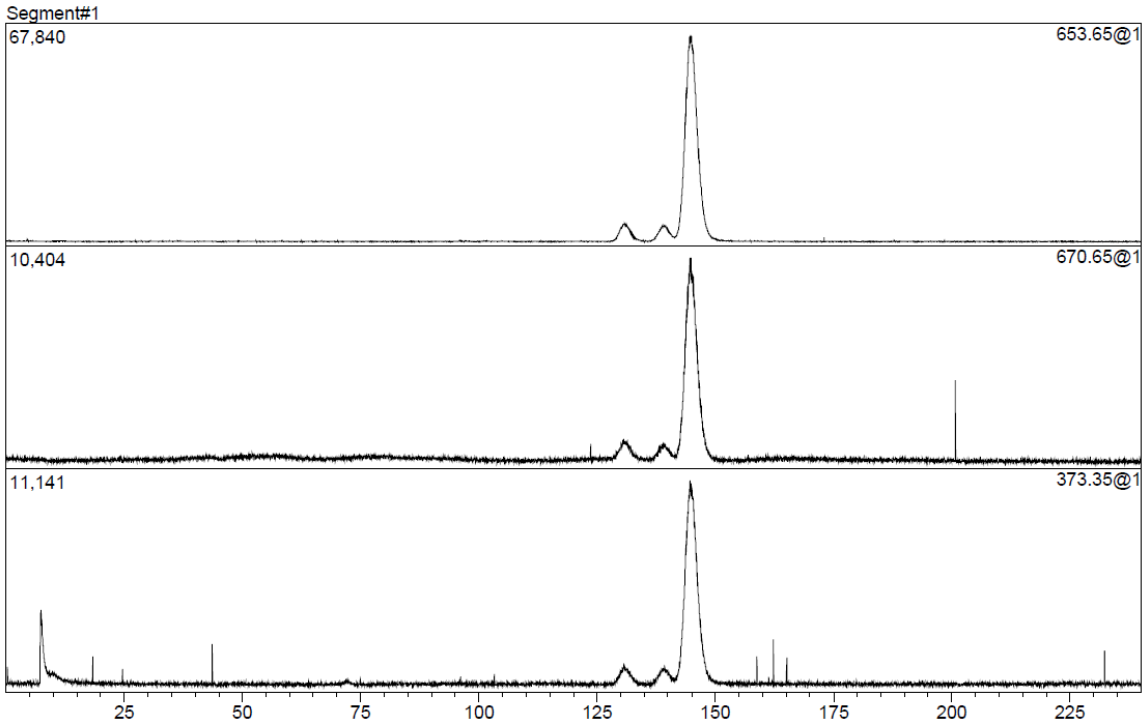

Figure S15. Total ion and extracted ion (m/z 653.65, 670.65 and 373.35) chromatograms for archaeol **2** (94% R) using chiral chromatography in polar organic mode. Methanol:H_2O 95:5% v/v was used as mobile phases at a flow of 0.4 mL/min with a post-column addition of 5 mM ammonium acetate at a flow of 0.1 mL/min.

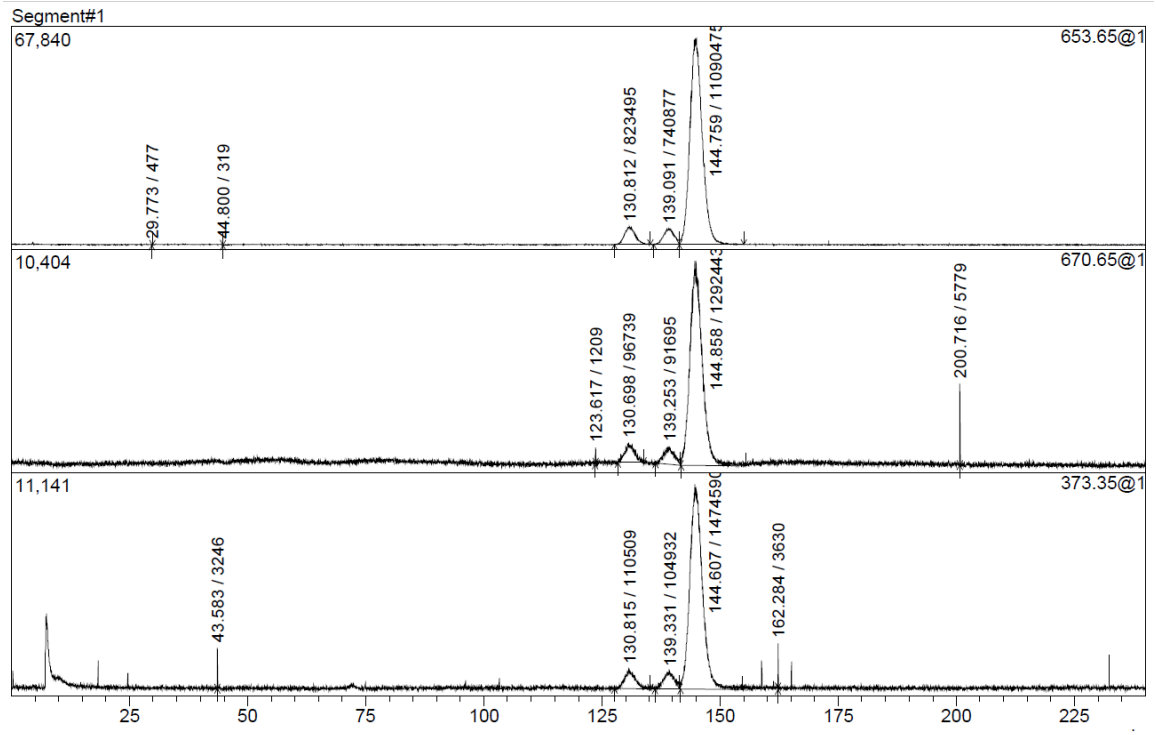

Ion m/z	Peak Area (S) RT: 130.8 min	Peak Area (R)a RT: 139.3 min	Peak Area (R)b RT: 144.8 min	Total Area	(%) R (a)	(%) R (b)	(%) R (total)	(%) S
653.65	823495	740877	11090475	12654847	5.85	87.64	93.5	6.51
760.65	96739	91695	1292443	1480877	6.19	87.28	93.5	6.53
373.35	110509	104932	1474590	1690031	6.21	87.25	93.5	6.54

Figure S16. HPLC chiral purity of R and S isomers of archaeol **2** using chiral chromatography in reverse mode. Methanol:H_2O 95:5% v/v was used as mobile phases at a flow of 0.4 mL/min with a post-column addition of 5 mM ammonium acetate at a flow of 0.1 mL/min.

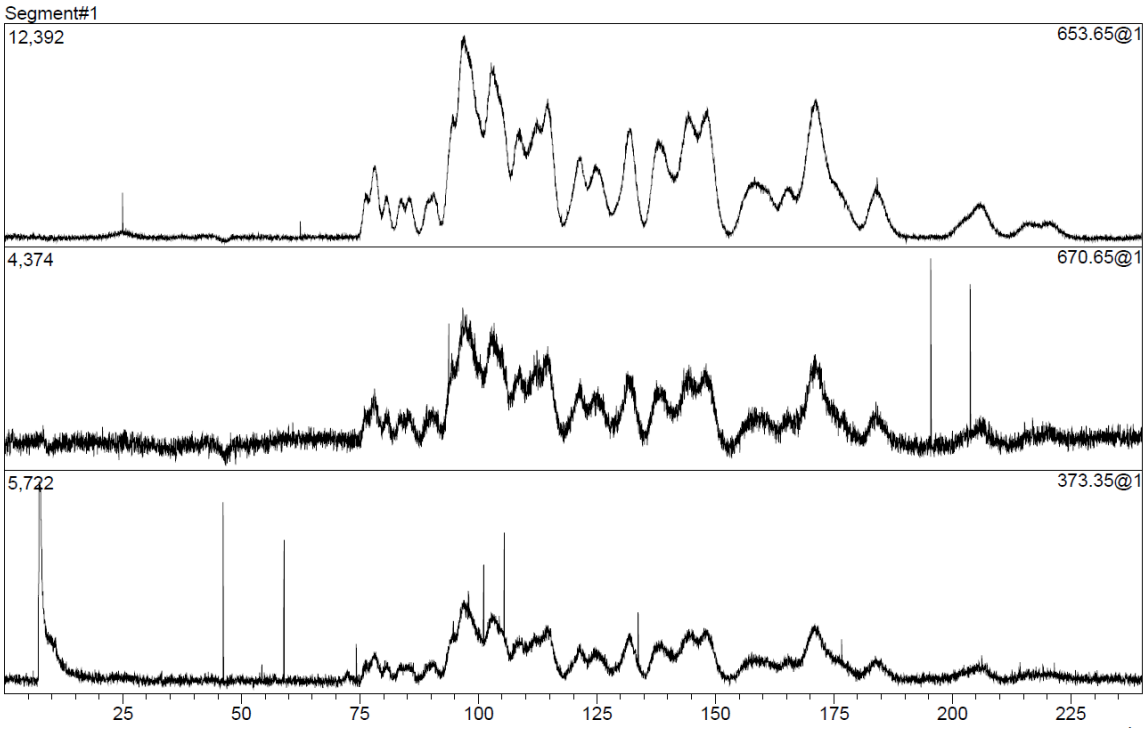

Figure S17. Total ion and extracted ion (m/z 653.65, 670.65 and 373.35) chromatograms for archaeol **3** (mixture of stereoisomers) using chiral chromatography in reverse mode. Methanol:H_2O 95:5% v/v was used as mobile phases at a flow of 0.4 mL/min with a post-column addition of 5 mM ammonium acetate at a flow of 0.1 mL/min.

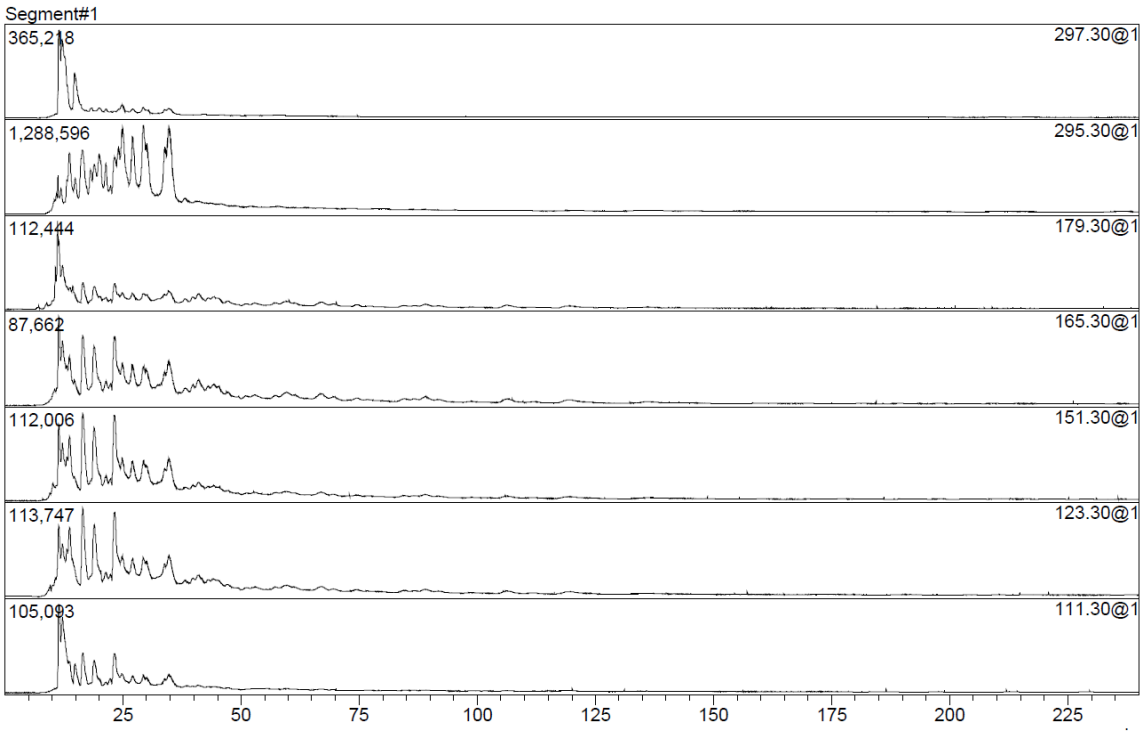

Figure S18. Total ion and extracted ion (molecular ion $[M+H]^+$ at m/z 297.3, reported fragments 295, 278, 165, 151, 123 and 111) chromatograms for phytol **7** using chiral chromatography in reverse mode. Methanol:H_2O 95:5% v/v was used as mobile phases at a flow of 0.4 mL/min with a post-column addition of 5 mM ammonium acetate at a flow of 0.1 mL/min.

9. Chiral chromatography (reverse phase) for elucidation of stereoisomers

An effort was made to have better separation between peaks. Phytol **7** (97% mixture of isomers) was analyzed and the molecular ion $[M+H]^+$ at m/z 297.3152, reported fragments 295, 278, 165, 151, 123 and 111, were also monitored. A single quadrupole mass spectrometer was used for detection and was set to Selected Ion Mass (SIM) and operated in positive ionization mode. The chromatograms showed more than 15 peaks for the same molecular ion $[M+H]^+$ at m/z 297.30 and reported fragments. This correlates with the highly complex chiral structure observed in the chiral chromatography of optically inactive archaeol **3.** Better peak separation was achieved using this method.

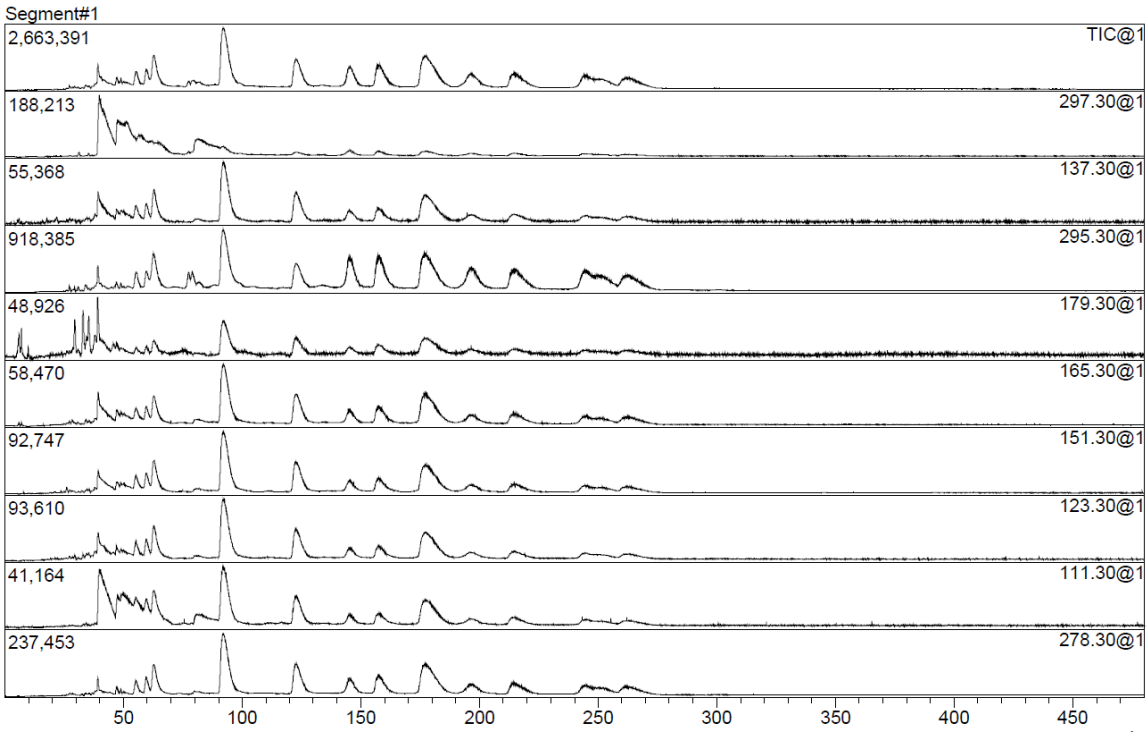

Figure S19. Total ion and extracted ion (Molecular ion $[M+H]^+$ at m/z 297.30, reported fragments 295, 278, 165, 151, 123 and 111) chromatograms for phytol **7** using chiral chromatography in reverse mode. Methanol:H_2O 85:15% v/v was used as mobile phases at a flow of 0.4 mL/min with a post-column addition of 5 mM ammonium acetate at a flow of 0.1 mL/min.

10. Percentage of archaeol 3 in 100% R configuration

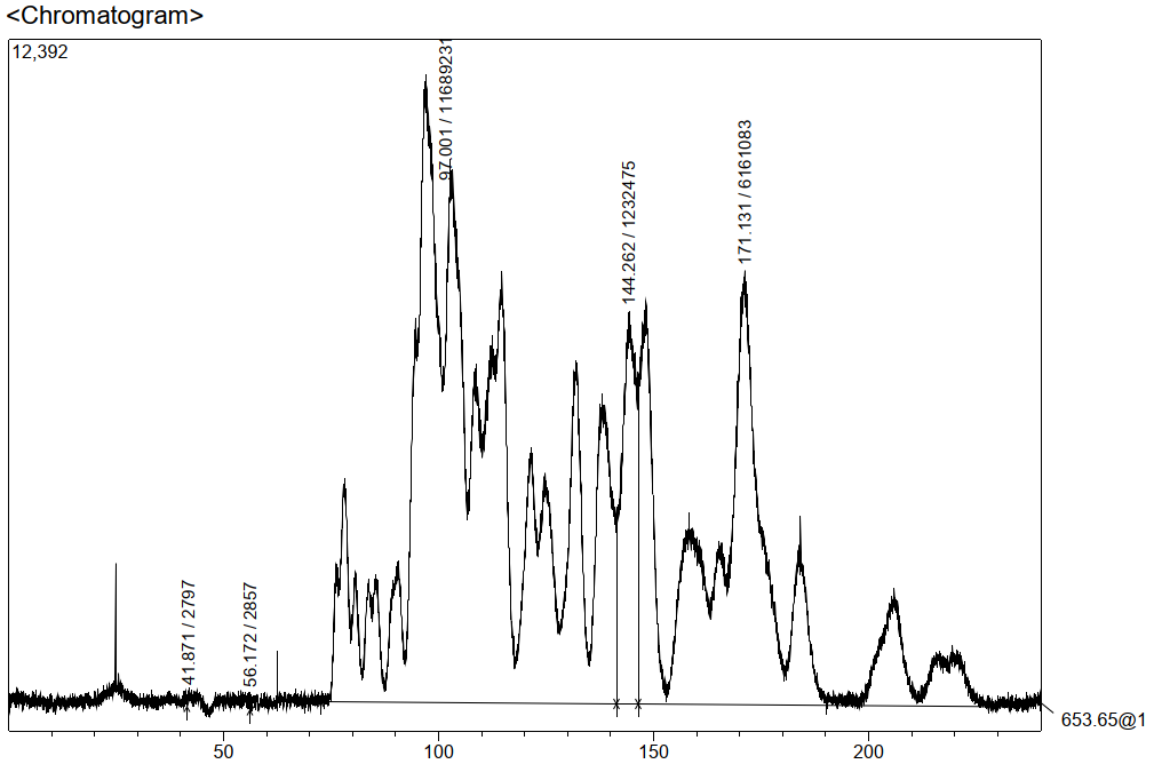

Figure S20: Chromatogram obtained from the chiral chromatography of optically inactive archaeol **3**, displaying a highly complex chiral composition with more than 20 peaks for the same molecular ion $[M+H]^+$ at m/z 653.65.

Table S2. Calculation of the percentage of archaeol 3 in the 100% R configuration

Ion m/z	Total Peak Area before R	Total Peak Area after R	Peak Area (R) RT: 144.2 min	Total Area	% of (R)-2,3-bis(((3R,7R,11R)-3,7,11,15-tetramethylhexadecyl)oxy) propan-1-ol (Archaeol **1**)
653.65	11689231	6161083	1232475	19082789	6.46%

This chromatogram was used to estimate the percentage of archaeol **3** corresponding to the single stereoisomer of archaeol **1**. It was determined by dividing the peak area of archaeol **3** at 144.2 minutes by the total area for all peaks (Table S2). Approximately 6.5% of archaeol **3** was found to have the 100% R configuration. It can therefore be extrapolated that while 100% of SLA contains 100% of archaeol **3**, 100% of **SLA-3** only contains about

6.5% of archaeol **1**. The remaining 93.5% of **SLA-3** contains other steoreoisomers of archaeol.

Compound 5

^{1}H NMR (500 MHz.

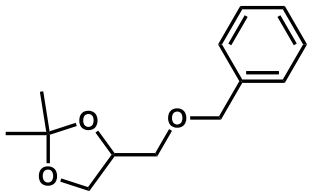

Compound 5

^{13}C NMR (126 MHz, $CDCl_3$)

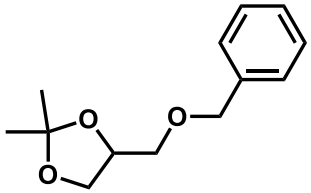

Compound 6

^{1}H NMR (500 MHz, $CDCl_3$)

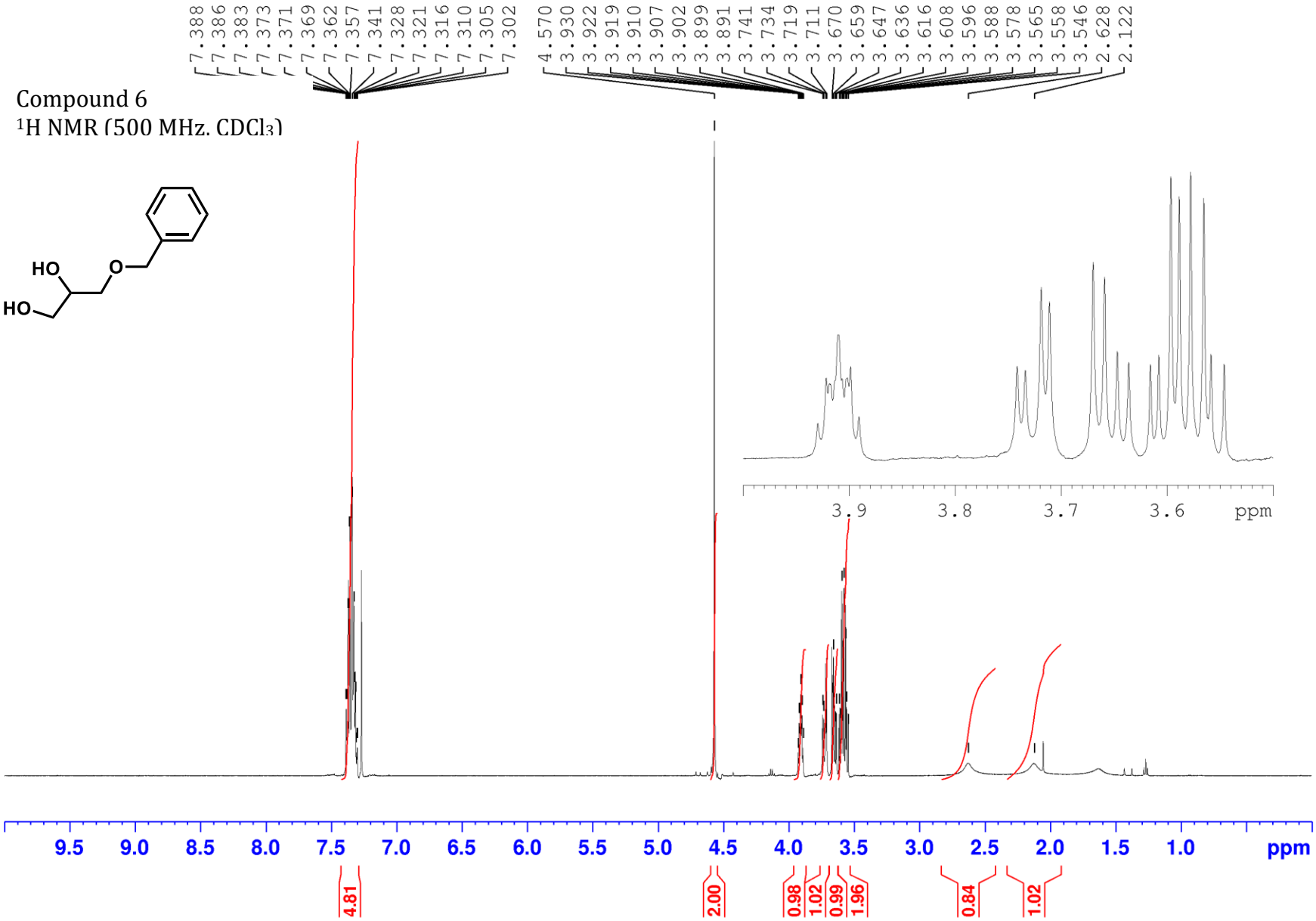

Compound 6

^{13}C NMR (176 MHz, $CDCl_3$)

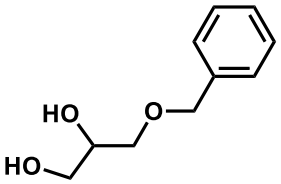

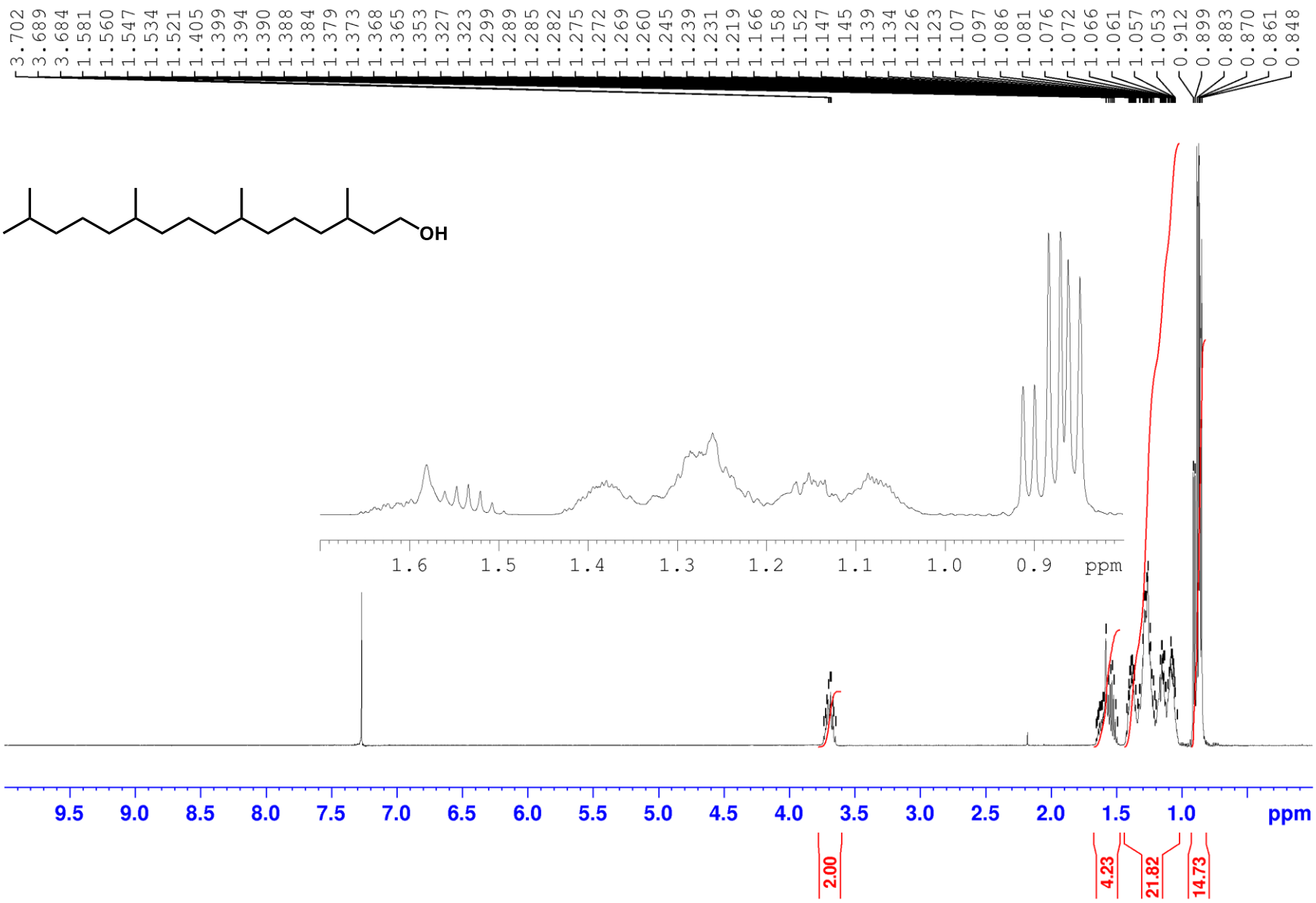
3.702
3.689
3.684
1.581
1.560
1.547
1.534
1.521
1.405
1.399
1.394
1.390
1.388
1.384
1.379
1.373
1.368
1.365
1.353
1.327
1.323
1.299
1.289
1.285
1.282
1.275
1.272
1.269
1.260
1.245
1.239
1.231
1.219
1.166
1.158
1.152
1.147
1.145
1.139
1.134
1.126
1.123
1.107
1.097
1.086
1.081
1.076
1.072
1.066
1.061
1.057
1.053
0.912
0.899
0.883
0.870
0.861
0.848
OH
1.6
1.5
1.4
1.3
1.2
1.1
1.0
0.9
ppm
9.5
9.0
8.5
8.0
7.5
7.0
6.5
6.0
5.5
5.0
4.5
4.0
3.5
3.0
2.5
2.0
1.5
1.0
ppm
2.00
4.23
21.82
14.73

Compound 8

^{13}C NMR (176 MHz, $CDCl_3$)

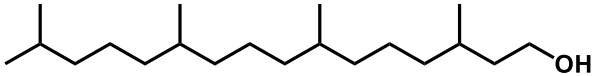

Compound 9

^{1}H NMR (500 MHz, $CDCl_3$)

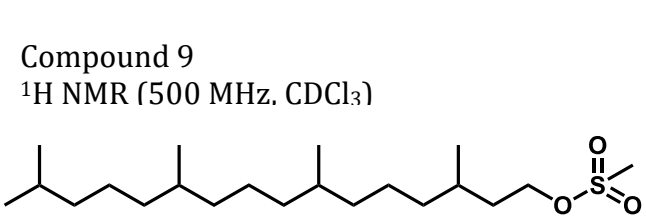

Compound 9

^{13}C NMR (176 MHz, $CDCl_3$)

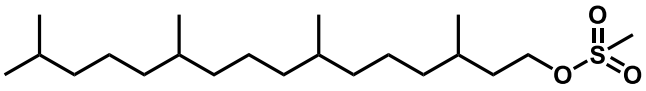

Compound 10

^{1}H NMR (500 MHz, $CDCl_3$)

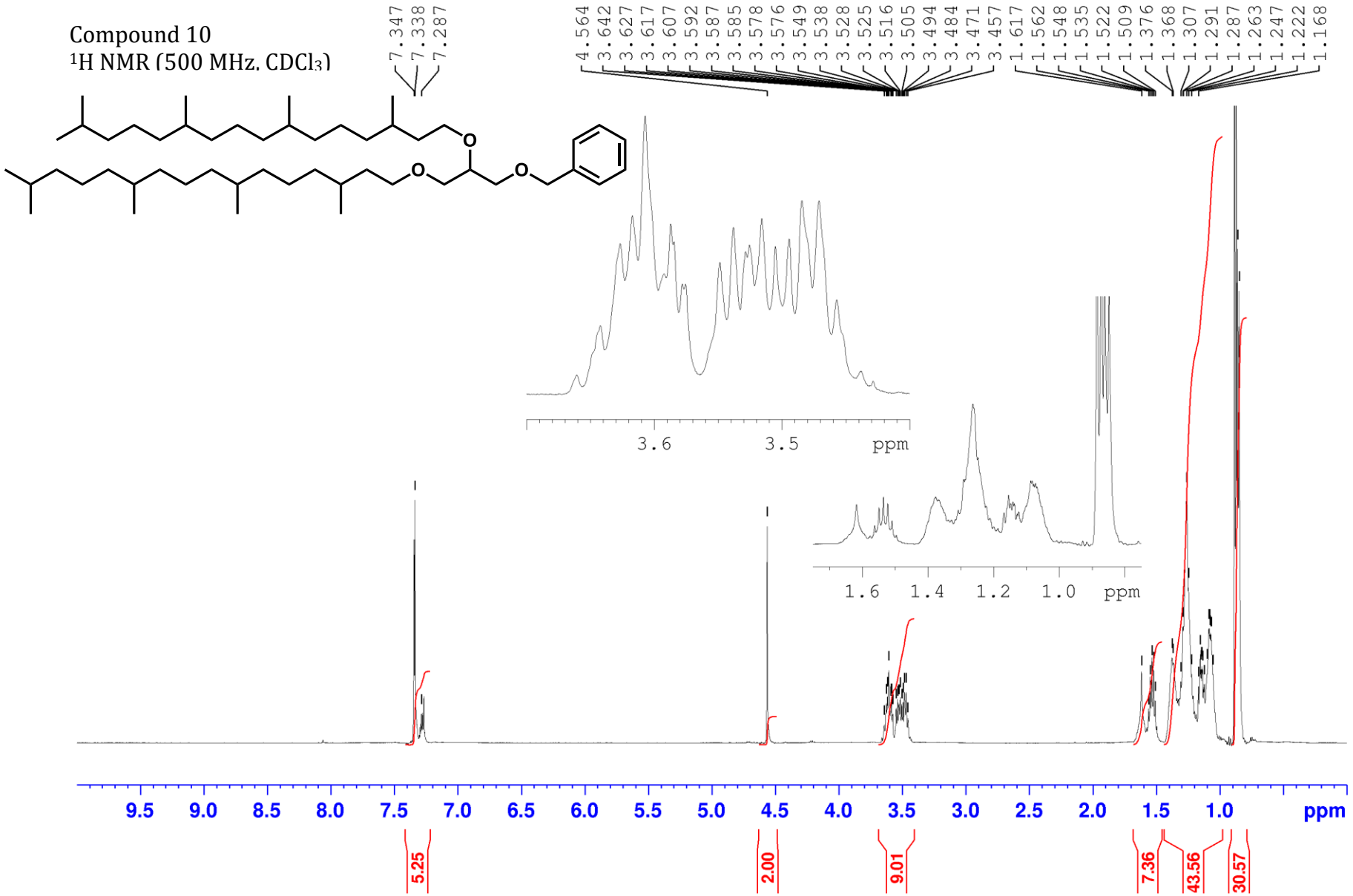

Compound 10

^{13}C NMR (176 MHz, $CDCl_3$)

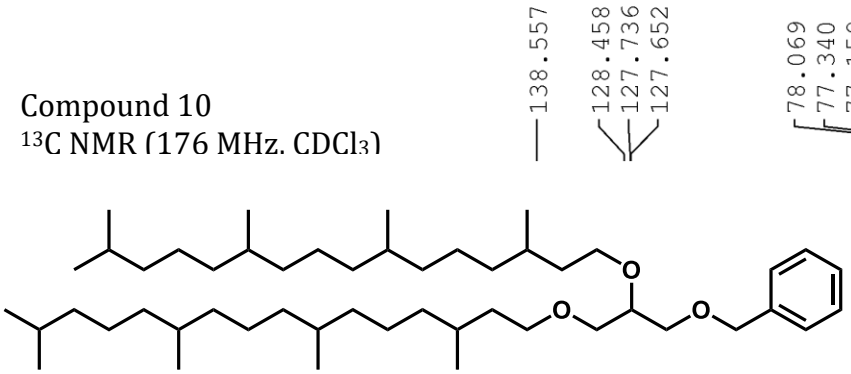

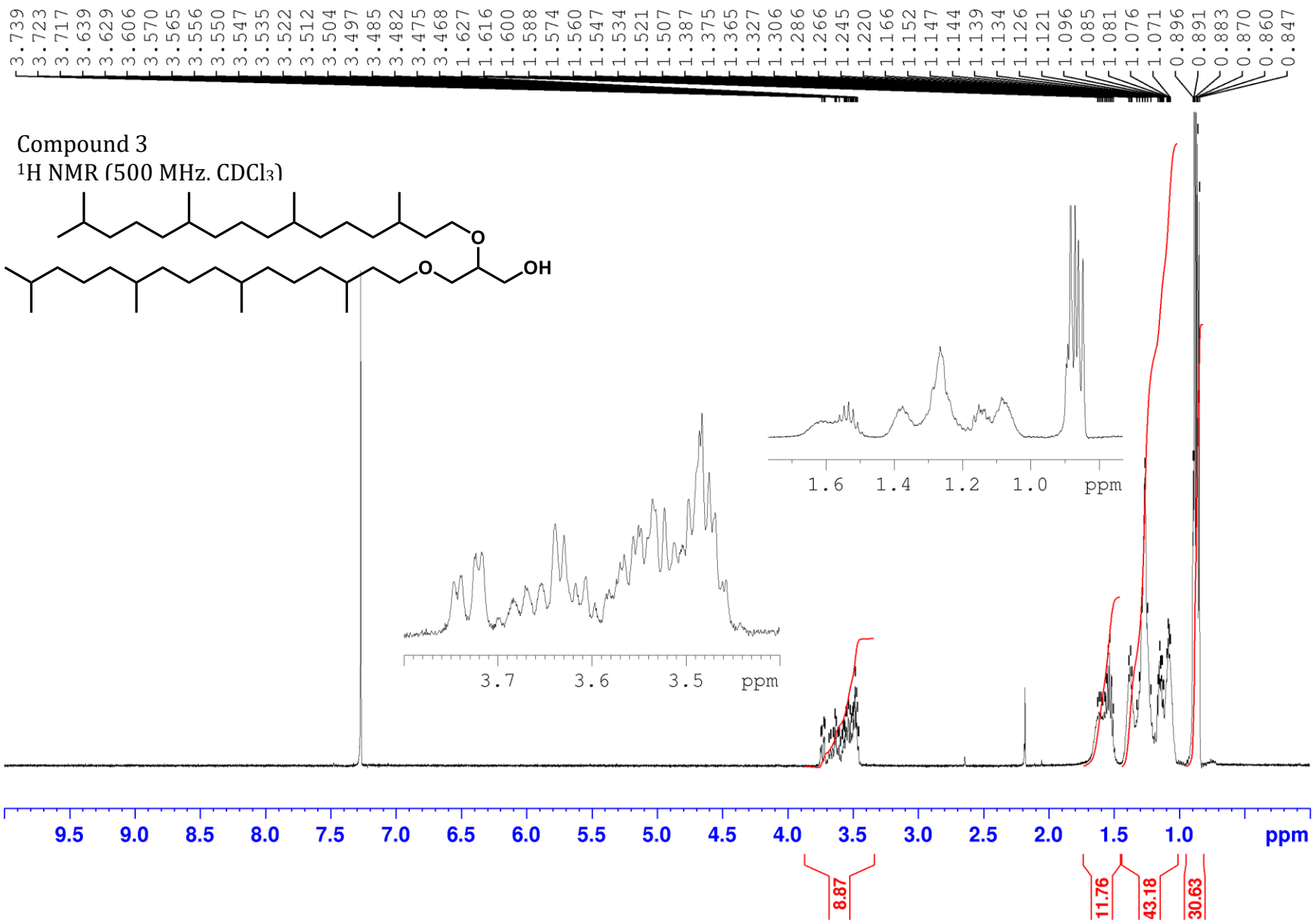
3.739
3.723
3.717
3.639
3.629
3.606
3.570
3.565
3.556
3.550
3.547
3.535
3.522
3.512
3.504
3.497
3.485
3.482
3.475
3.468
1.627
1.616
1.600
1.588
1.574
1.560
1.547
1.534
1.521
1.507
1.387
1.375
1.365
1.327
1.306
1.286
1.266
1.245
1.220
1.166
1.152
1.147
1.144
1.139
1.134
1.126
1.121
1.096
1.085
1.081
1.076
1.071
0.896
0.891
0.883
0.870
0.860
0.847
Compound 3
1H NMR (500 MHz, CDCl3)
O
O
OH
3.7
3.6
3.5
ppm
1.6
1.4
1.2
1.0
ppm
9.5
9.0
8.5
8.0
7.5
7.0
6.5
6.0
5.5
5.0
4.5
4.0
3.5
3.0
2.5
2.0
1.5
1.0
ppm
8.87
11.76
43.18
30.63

Compound 3

^{13}C NMR (176 MHz, $CDCl_3$)

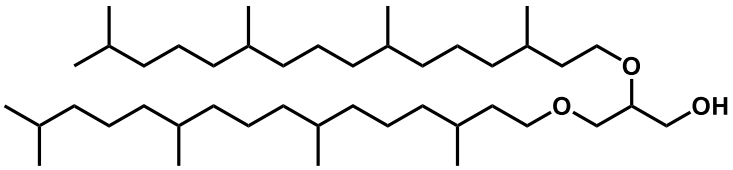

78.390
78.375
78.367
77.340
77.159
76.978
71.152
71.131
71.089
71.063
70.304
68.802
68.782
63.271
63.248
39.504
37.637
37.625
37.605
37.591
37.559
37.543
37.529
37.485
37.461
37.427
37.276
37.267
37.195
37.185
36.799
36.713
32.939
32.920
30.015

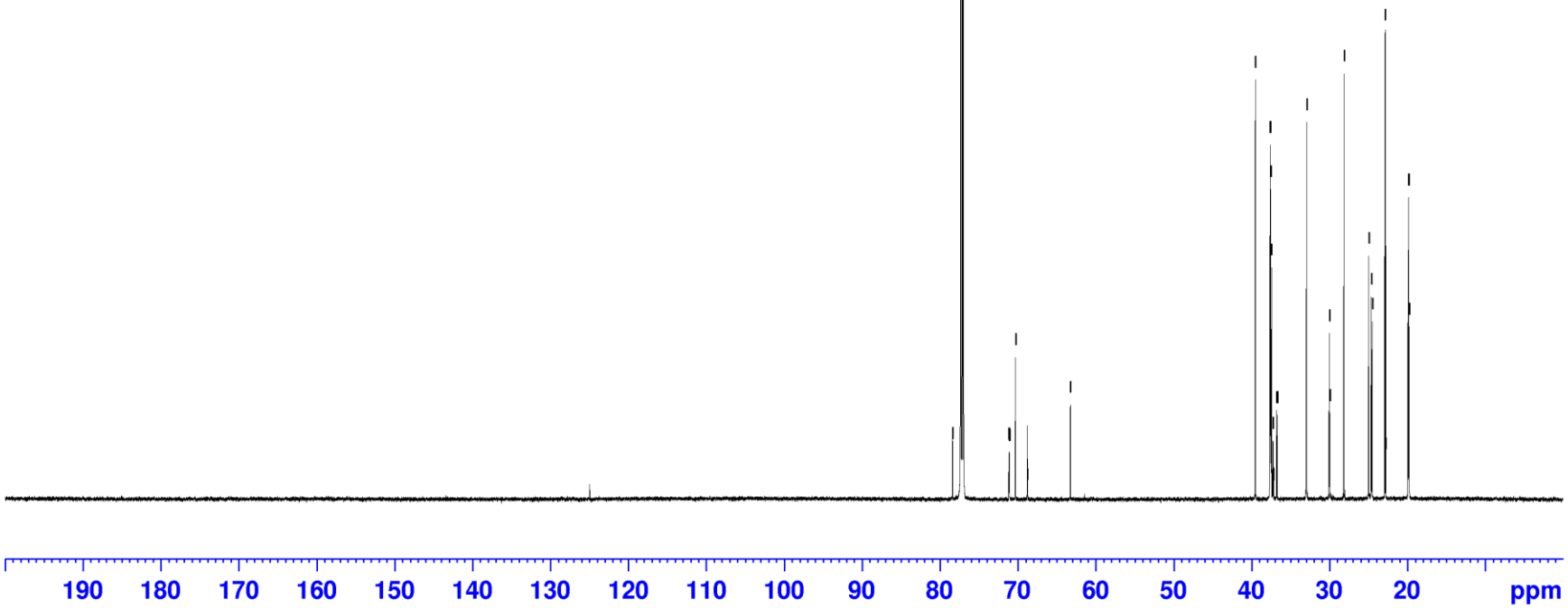

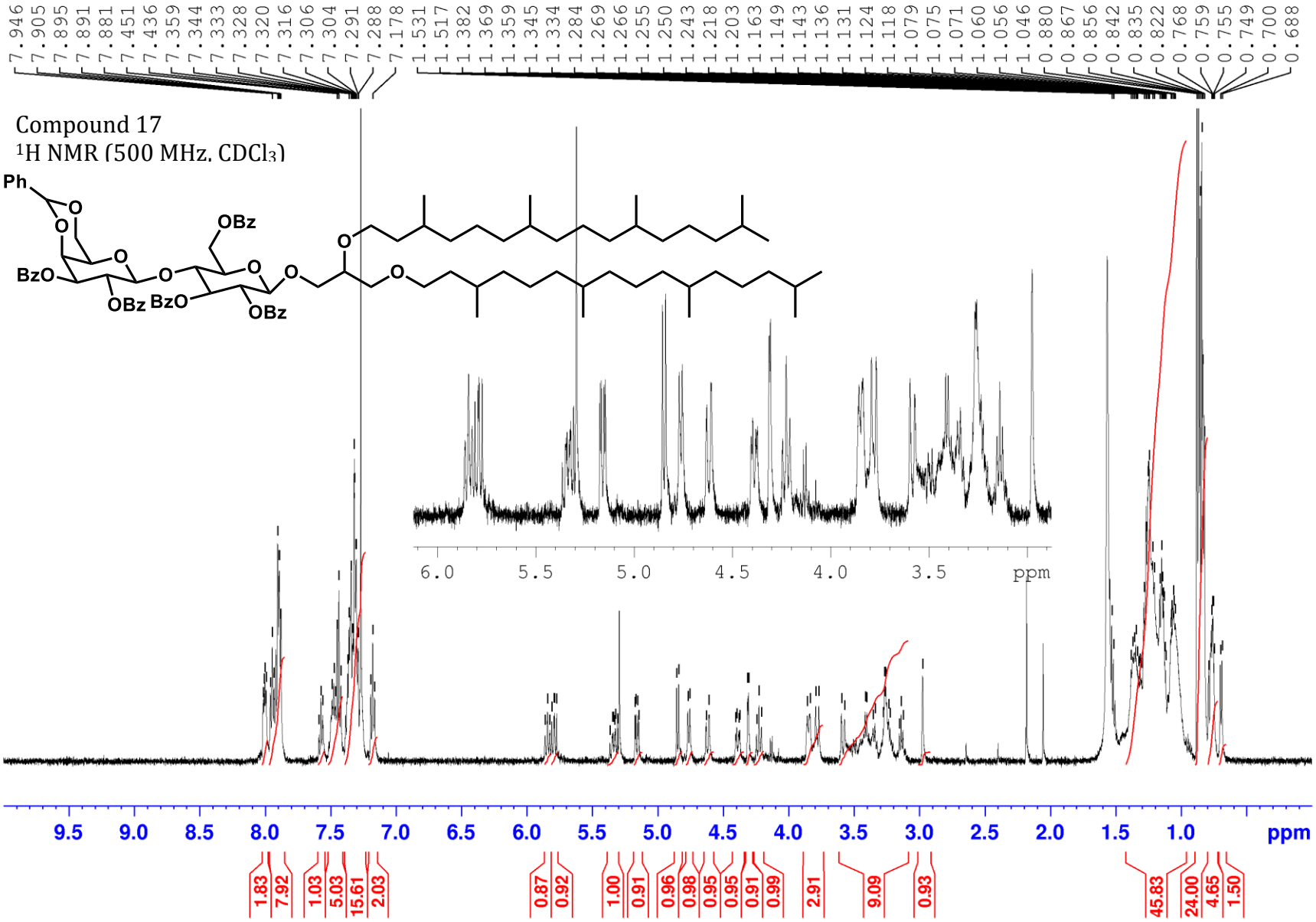
7.946 7.905 7.895 7.891 7.881 7.451 7.436 7.359 7.344 7.333 7.328 7.320 7.316 7.306 7.304 7.291 7.288 7.178
1.531 1.517 1.382 1.369 1.359 1.345 1.334 1.284 1.269 1.266 1.255 1.250 1.243 1.218 1.203 1.163 1.149 1.143 1.136 1.131 1.124 1.118 1.079 1.075 1.071 1.060 1.056 1.046 0.880 0.867 0.856 0.842 0.835 0.822 0.768 0.759 0.755 0.749 0.700 0.688
Compound 17
1H NMR (500 MHz, CDCl3)
Ph
BzO
OBz
OBz
BzO
OBz
6.0 5.5 5.0 4.5 4.0 3.5 ppm
9.5 9.0 8.5 8.0 7.5 7.0 6.5 6.0 5.5 5.0 4.5 4.0 3.5 3.0 2.5 2.0 1.5 1.0 ppm
1.83 7.92 1.03 5.03 15.61 2.03 0.87 0.92 1.00 0.91 0.96 0.98 0.95 0.95 0.91 0.99 2.91 9.09 0.93 45.83 24.00 4.65 1.50

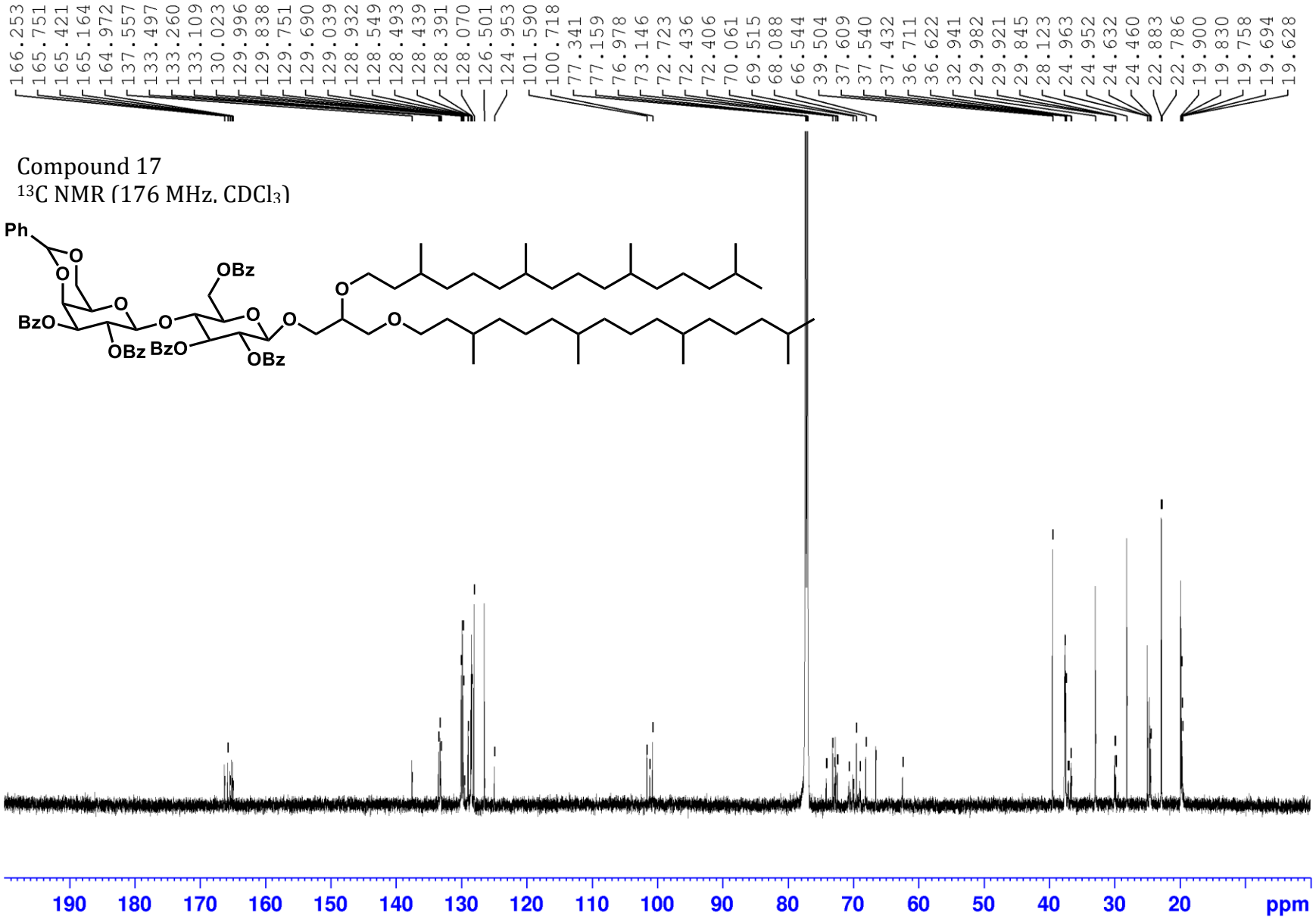
166.253
165.751
165.421
165.164
164.972
137.557
133.497
133.260
133.109
130.023
129.996
129.838
129.751
129.690
129.039
128.932
128.549
128.493
128.439
128.391
128.070
126.501
124.953
101.590
100.718
77.341
77.159
76.978
73.146
72.723
72.436
72.406
70.061
69.515
68.088
66.544
39.504
37.609
37.540
37.432
36.711
36.622
32.941
29.982
29.921
29.845
28.123
24.963
24.952
24.632
24.460
22.883
22.786
19.900
19.830
19.758
19.694
19.628
Compound 17
13C NMR (176 MHz, CDCl3)
Ph
O
O
OBz
BzO
O
O
O
O
O
O
OBz
BzO
OBz
190
180
170
160
150
140
130
120
110
100
90
80
70
60
50
40
30
20
ppm

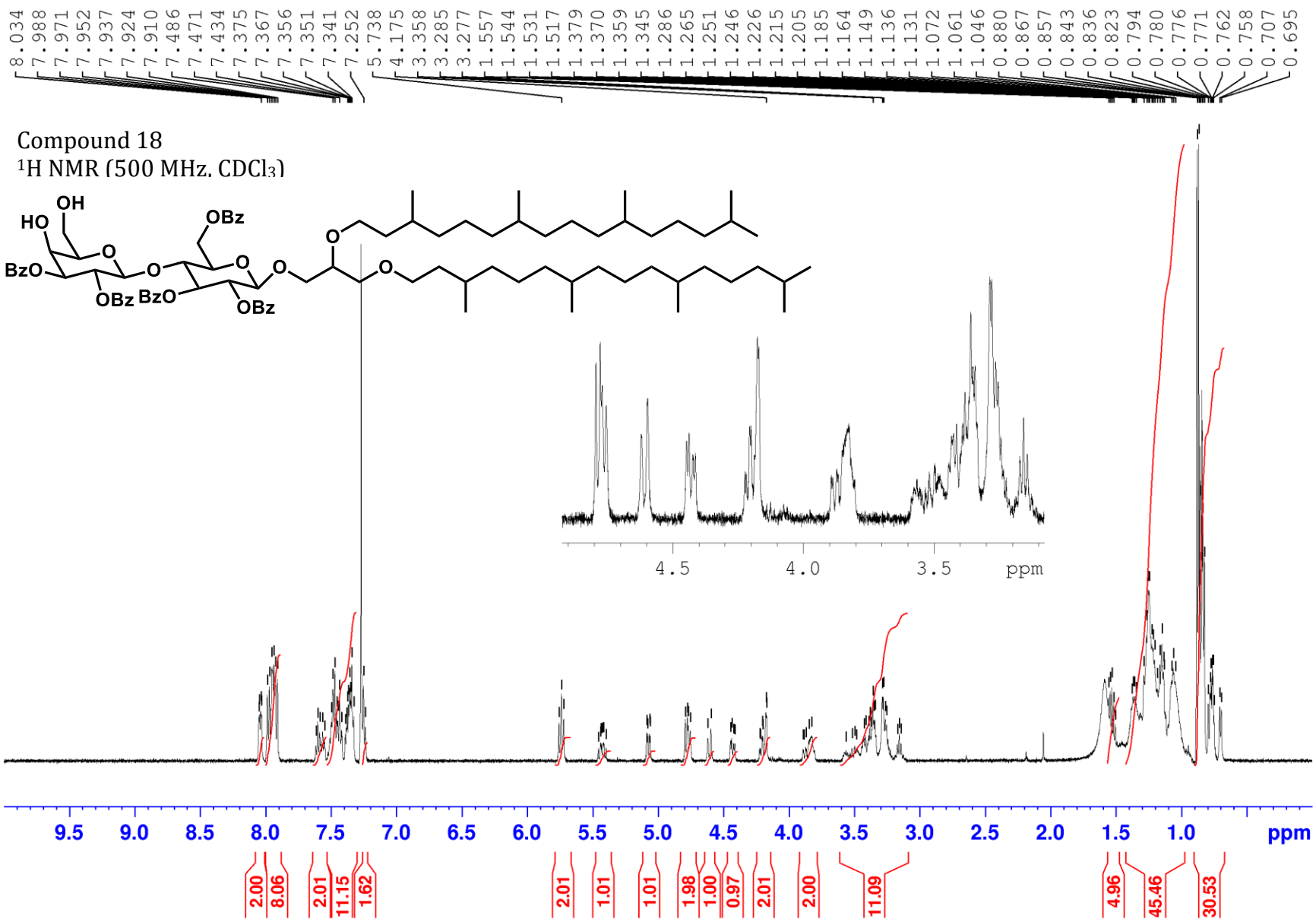
8.034
7.988
7.971
7.952
7.937
7.924
7.910
7.486
7.471
7.434
7.375
7.367
7.356
7.351
7.341
7.252
5.738
4.175
3.358
3.285
3.277
1.557
1.544
1.531
1.517
1.379
1.370
1.359
1.345
1.286
1.265
1.251
1.246
1.226
1.215
1.205
1.185
1.164
1.149
1.136
1.131
1.072
1.061
1.046
0.880
0.867
0.857
0.843
0.836
0.823
0.794
0.780
0.776
0.771
0.762
0.758
0.707
0.695
Compound 18
1H NMR (500 MHz, CDCl3)
OH
HO
OBz
O
BzO
O
O
O
O
OBz
BzO
OBz
4.5
4.0
3.5
ppm
9.5
9.0
8.5
8.0
7.5
7.0
6.5
6.0
5.5
5.0
4.5
4.0
3.5
3.0
2.5
2.0
1.5
1.0
ppm
2.00
8.06
2.01
11.15
1.62
2.01
1.01
1.01
1.98
1.00
0.97
2.01
2.00
11.09
4.96
45.46
30.53

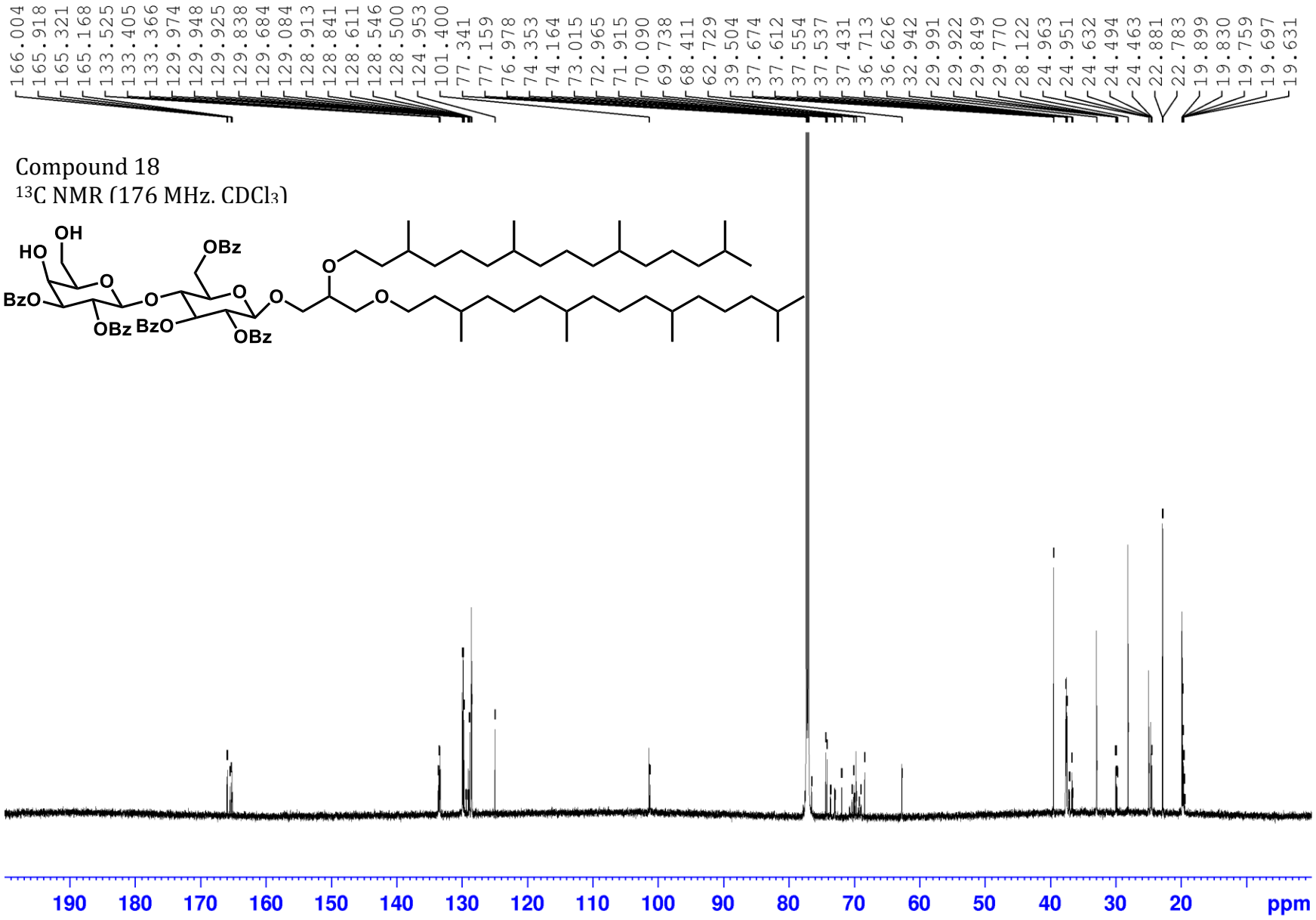
166.004
165.918
165.321
165.168
133.525
133.405
133.366
129.974
129.948
129.925
129.838
129.684
129.084
128.913
128.841
128.611
128.546
128.500
124.953
101.400
77.341
77.159
76.978
74.353
74.164
73.015
72.965
71.915
70.090
69.738
68.411
62.729
39.504
37.674
37.612
37.554
37.537
37.431
36.713
36.626
32.942
29.991
29.922
29.849
29.770
28.122
24.963
24.951
24.632
24.494
24.463
22.881
22.783
19.899
19.830
19.759
19.697
19.631
Compound 18
13C NMR (176 MHz, CDCl3)
OH
HO
OBz
BzO
OBz
BzO
OBz
O
190
180
170
160
150
140
130
120
110
100
90
80
70
60
50
40
30
20
ppm

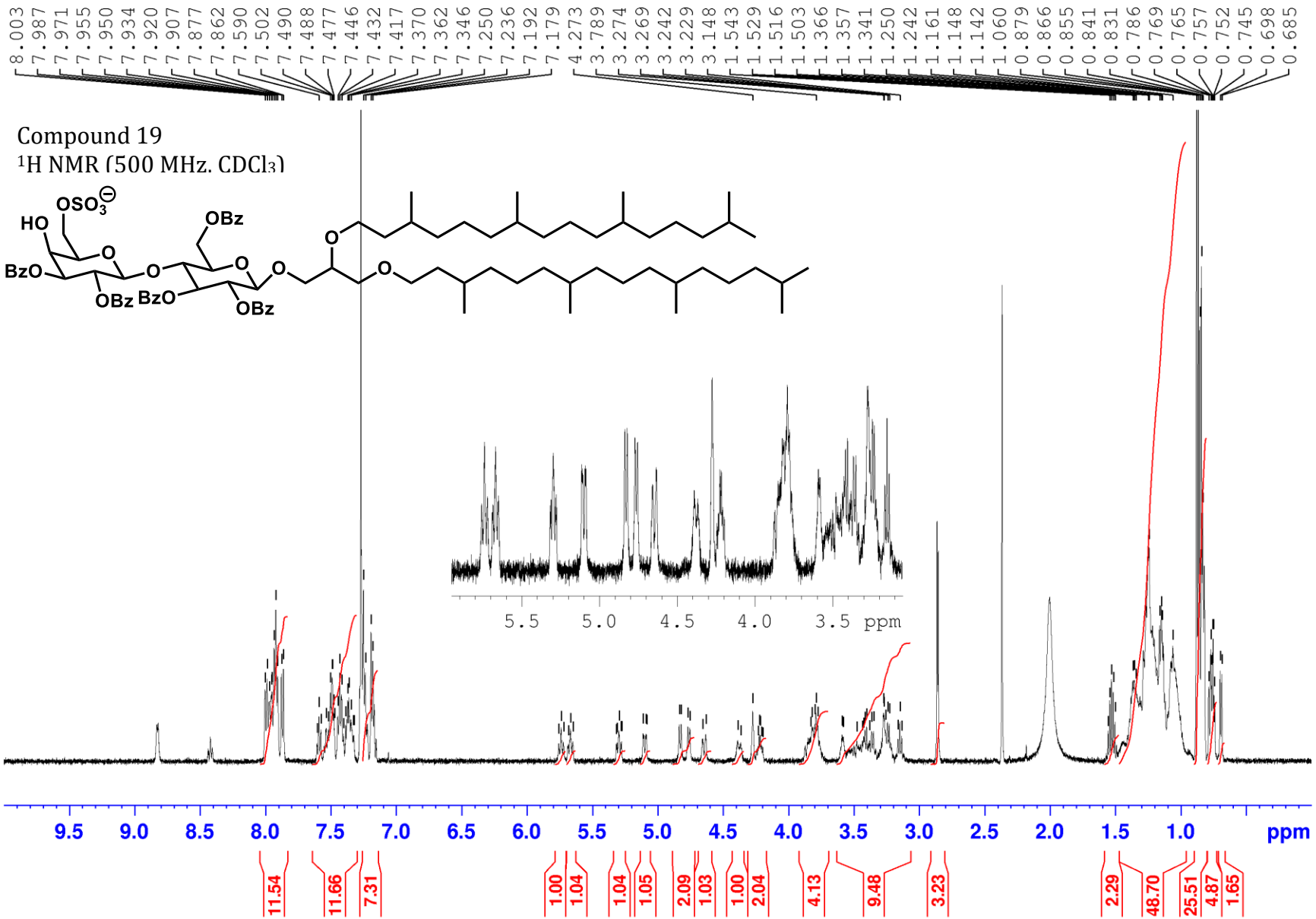
8.003
7.987
7.971
7.955
7.950
7.934
7.920
7.907
7.877
7.862
7.590
7.502
7.490
7.488
7.477
7.446
7.432
7.417
7.370
7.362
7.346
7.250
7.236
7.192
7.179
4.273
3.789
3.274
3.269
3.242
3.229
3.148
1.543
1.529
1.516
1.503
1.366
1.357
1.341
1.250
1.242
1.161
1.148
1.142
1.060
0.879
0.866
0.855
0.841
0.831
0.786
0.769
0.765
0.757
0.752
0.745
0.698
0.685
Compound 19
1H NMR (500 MHz, CDCl3)
HO
OSO3
OBz
BzO
OBz
BzO
OBz
O
5.5
5.0
4.5
4.0
3.5
ppm
9.5
9.0
8.5
8.0
7.5
7.0
6.5
6.0
5.5
5.0
4.5
4.0
3.5
3.0
2.5
2.0
1.5
1.0
ppm
11.54
11.66
7.31
1.00
1.04
1.04
1.05
2.09
1.03
1.00
2.04
4.13
9.48
3.23
2.29
48.70
25.51
4.87
1.65

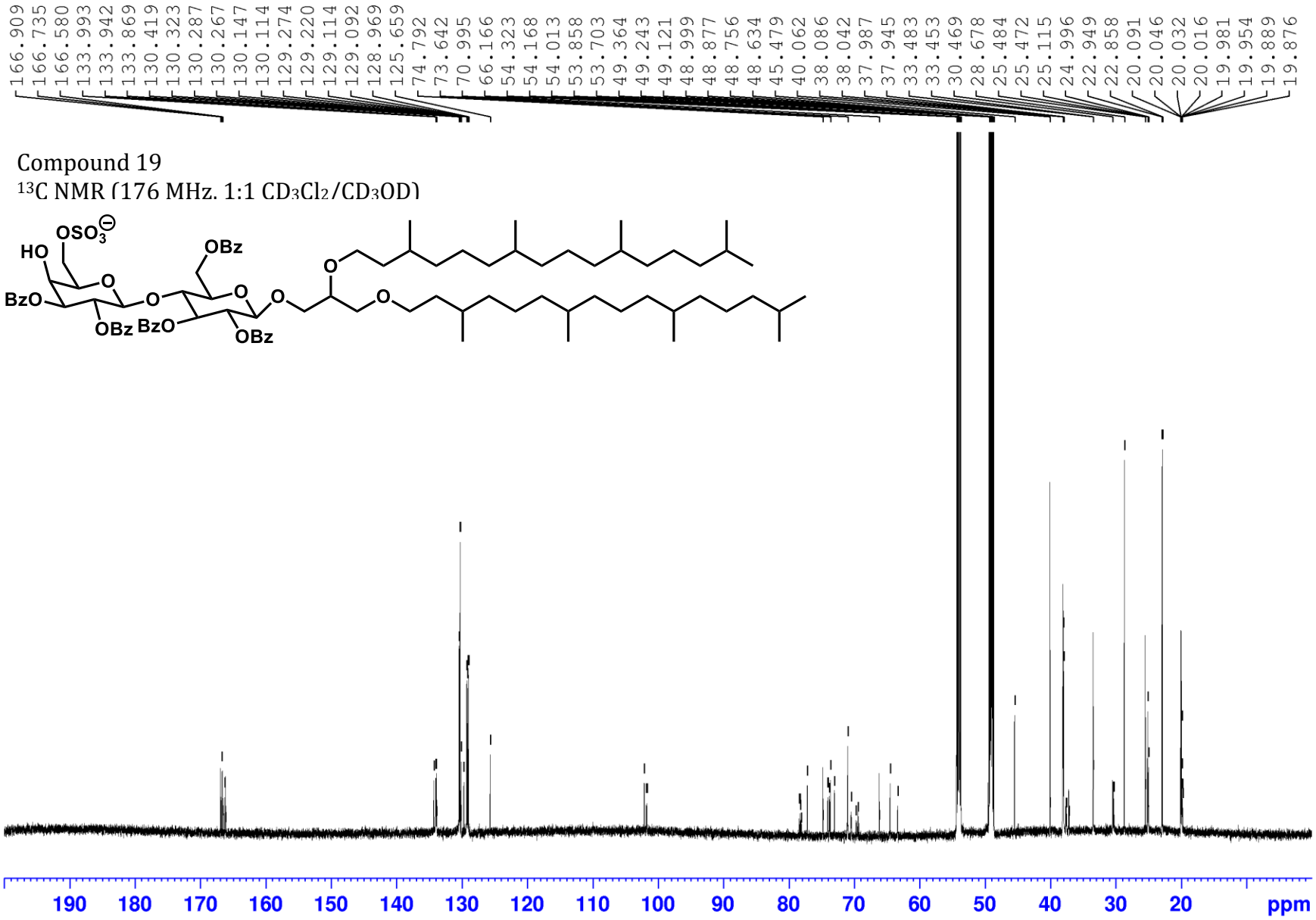
166.909
166.735
166.580
133.993
133.942
133.869
130.419
130.323
130.287
130.267
130.147
130.114
129.274
129.220
129.114
129.092
128.969
125.659
74.792
73.642
70.995
66.166
54.323
54.168
54.013
53.858
53.703
49.364
49.243
49.121
48.999
48.877
48.756
48.634
45.479
40.062
38.086
38.042
37.987
37.945
33.483
33.453
30.469
28.678
25.484
25.472
25.115
24.996
22.949
22.858
20.091
20.046
20.032
20.016
19.981
19.954
19.889
19.876
Compound 19
13C NMR (176 MHz, 1:1 CD3Cl2/CD3OD)
OSO3
HO
OBz
O
BzO
OBz
BzO
OBz
190
180
170
160
150
140
130
120
110
100
90
80
70
60
50
40
30
20
ppm

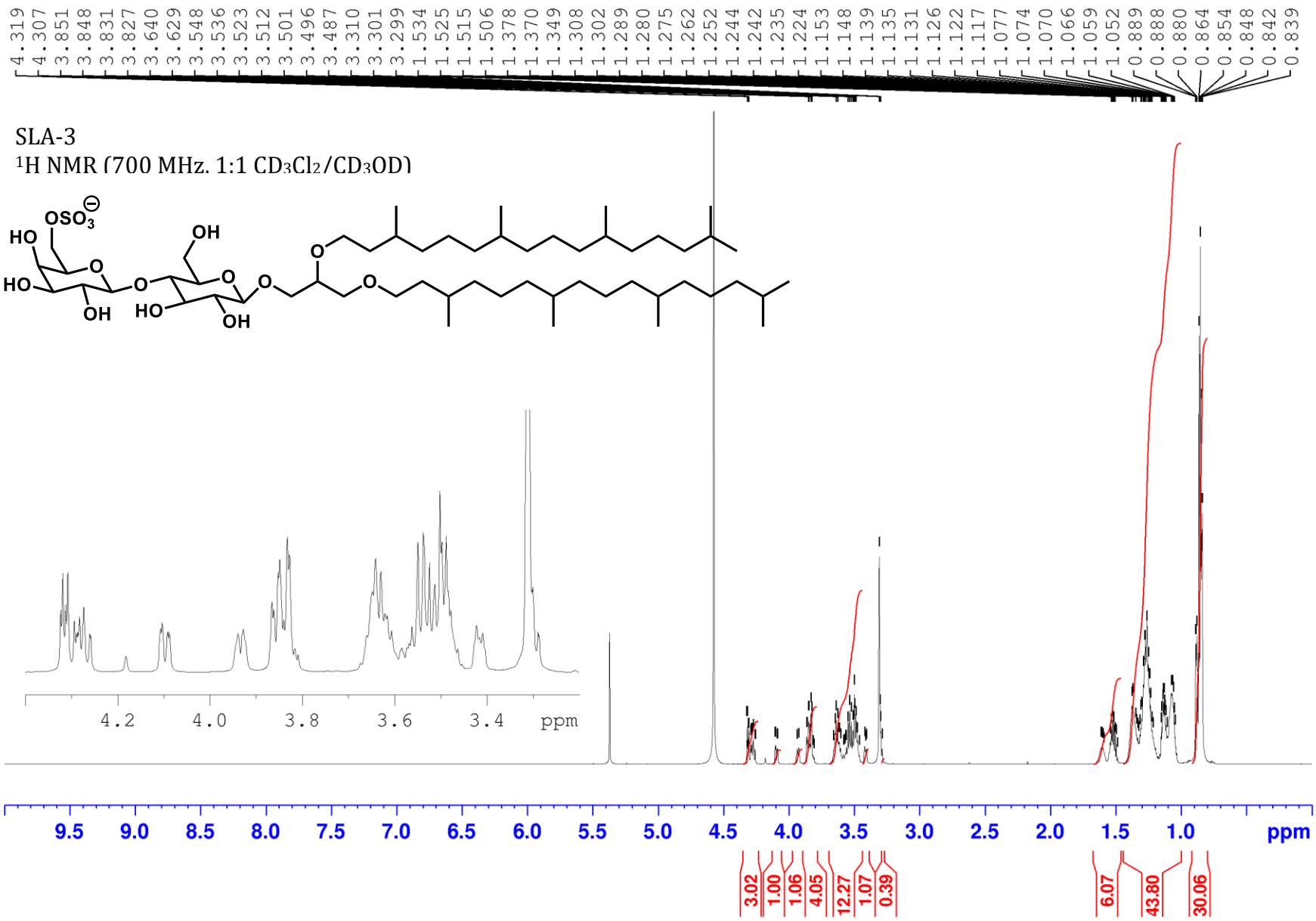
4.319
4.307
3.851
3.848
3.831
3.827
3.640
3.629
3.548
3.536
3.523
3.512
3.501
3.496
3.487
3.310
3.301
3.299
1.534
1.525
1.515
1.506
1.378
1.370
1.349
1.308
1.302
1.289
1.280
1.275
1.262
1.252
1.244
1.242
1.235
1.224
1.153
1.148
1.139
1.135
1.131
1.126
1.122
1.117
1.077
1.074
1.070
1.066
1.059
1.052
0.889
0.888
0.880
0.864
0.854
0.848
0.842
0.839
SLA-3
1H NMR (700 MHz, 1:1 CD3Cl2/CD3OD)
OSO3
HO
OH
HO
OH
HO
OH
O
O
O
O
O
O
4.2
4.0
3.8
3.6
3.4
ppm
9.5
9.0
8.5
8.0
7.5
7.0
6.5
6.0
5.5
5.0
4.5
4.0
3.5
3.0
2.5
2.0
1.5
1.0
ppm
3.02
1.00
1.06
4.05
12.27
1.07
0.39
6.07
43.80
30.06

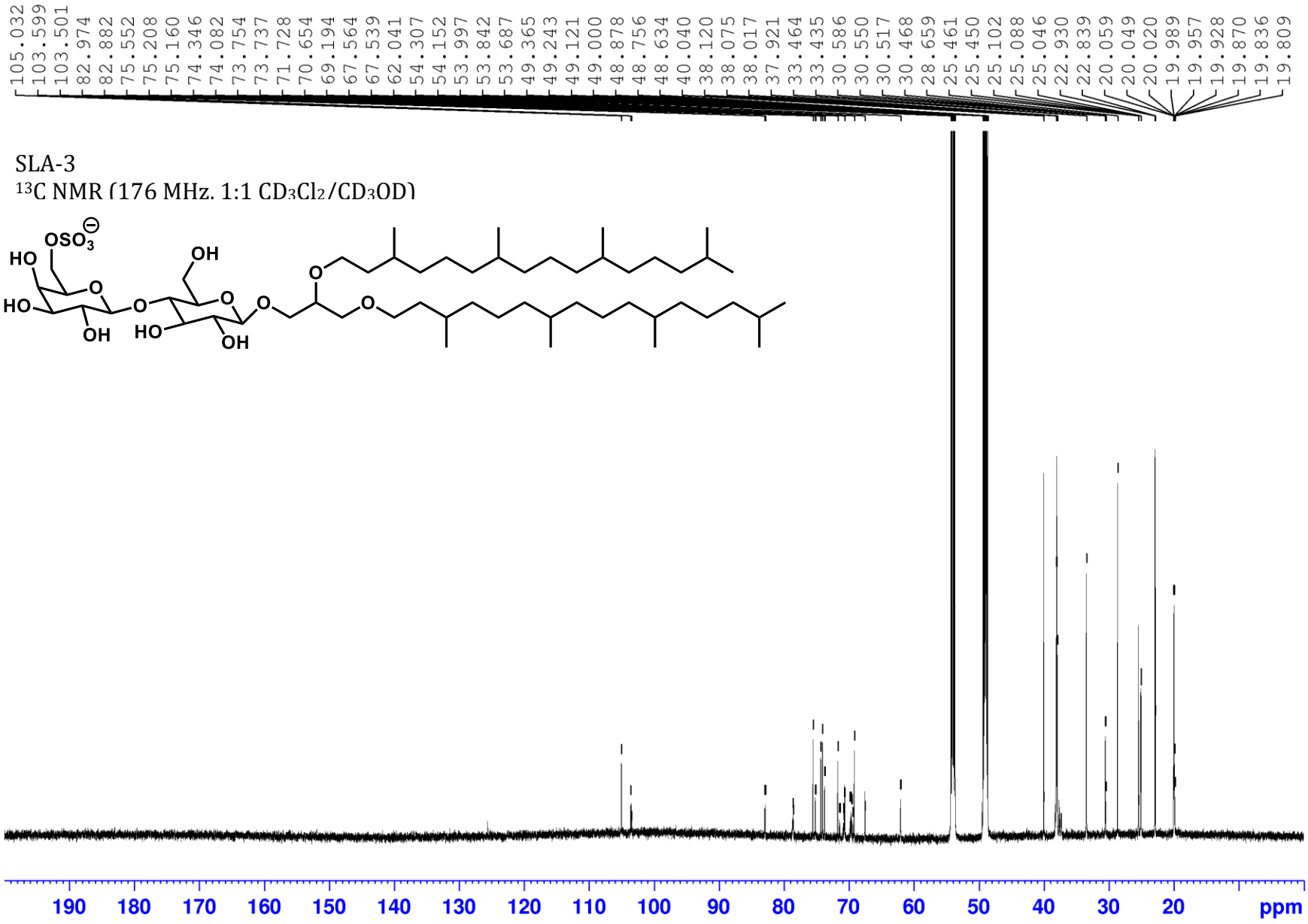
105.032
103.599
103.501
82.974
82.882
75.552
75.208
75.160
74.346
74.082
73.754
73.737
71.728
70.654
69.194
67.564
67.539
62.041
54.307
54.152
53.997
53.842
53.687
49.365
49.243
49.121
49.000
48.878
48.756
48.634
40.040
38.120
38.075
38.017
37.921
33.464
33.435
30.586
30.550
30.517
30.468
28.659
25.461
25.450
25.102
25.088
25.046
22.930
22.839
20.059
20.049
20.020
19.989
19.957
19.928
19.870
19.836
19.809
SLA-3
13C NMR (176 MHz, 1:1 CD3Cl2/CD3OD)
OSO3
HO
OH
O
HO
OH
O
O
HO
OH
O
O
O
190
180
170
160
150
140
130
120
110
100
90
80
70
60
50
40
30
20
ppm

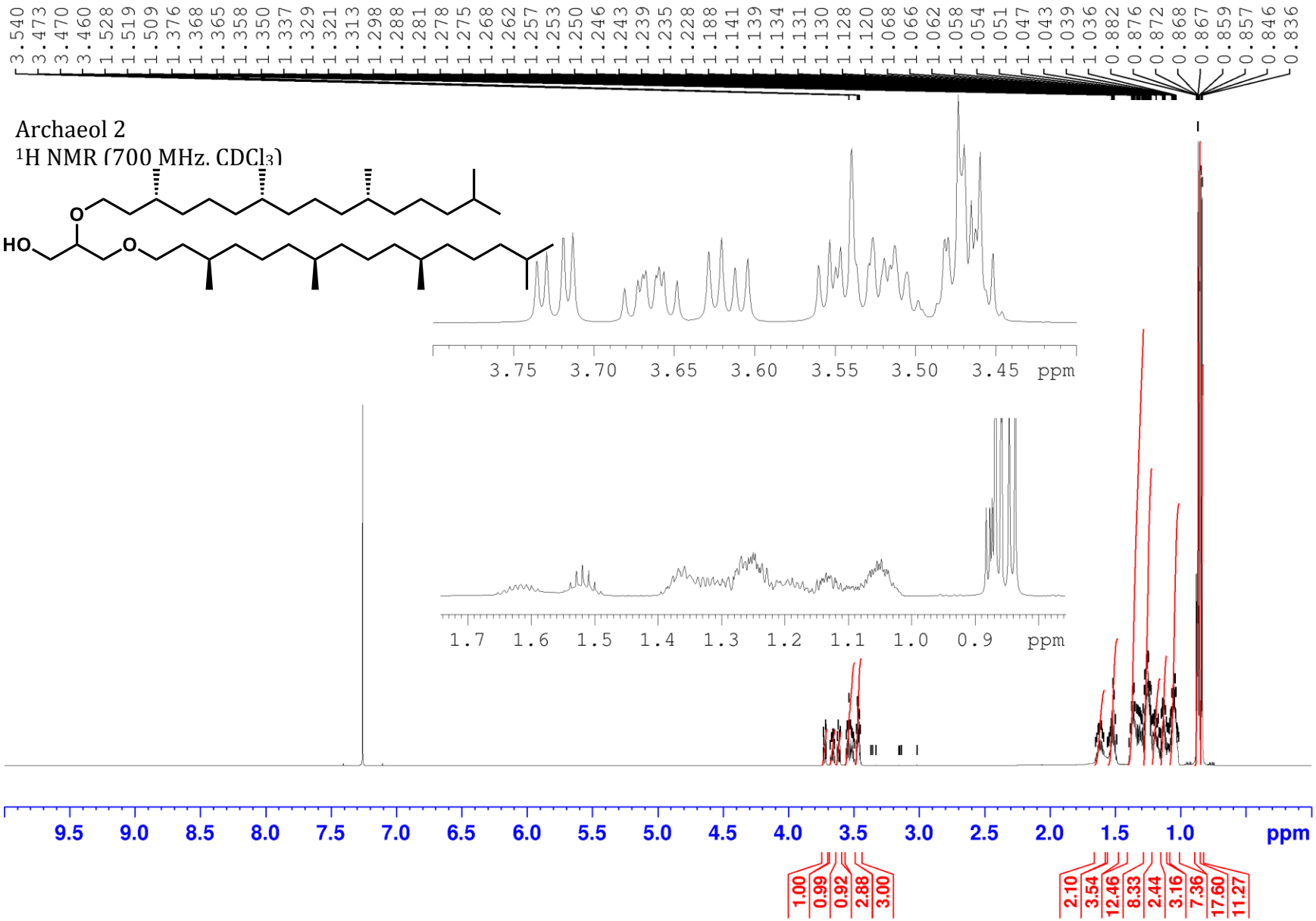
3.540
3.473
3.470
3.460
1.528
1.519
1.509
1.376
1.368
1.365
1.358
1.350
1.337
1.329
1.321
1.313
1.298
1.288
1.281
1.278
1.275
1.268
1.262
1.257
1.253
1.250
1.246
1.243
1.239
1.235
1.228
1.188
1.141
1.139
1.134
1.131
1.130
1.128
1.120
1.068
1.066
1.062
1.058
1.054
1.051
1.047
1.043
1.039
1.036
0.882
0.876
0.872
0.868
0.867
0.859
0.857
0.846
0.836
Archaeol 2
^{1}H NMR (700 MHz, $CDCl_3$)
HO
O
O
3.75
3.70
3.65
3.60
3.55
3.50
3.45
ppm
1.7
1.6
1.5
1.4
1.3
1.2
1.1
1.0
0.9
ppm
9.5
9.0
8.5
8.0
7.5
7.0
6.5
6.0
5.5
5.0
4.5
4.0
3.5
3.0
2.5
2.0
1.5
1.0
ppm
1.00
0.99
0.92
2.88
3.00
2.10
3.54
12.46
8.33
2.44
3.16
7.36
17.60
11.27

Archaeol 2

^{13}C NMR (176 MHz, $CDCl_3$)

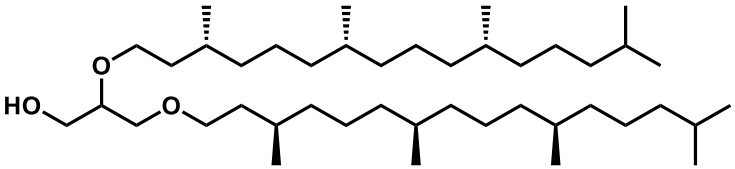

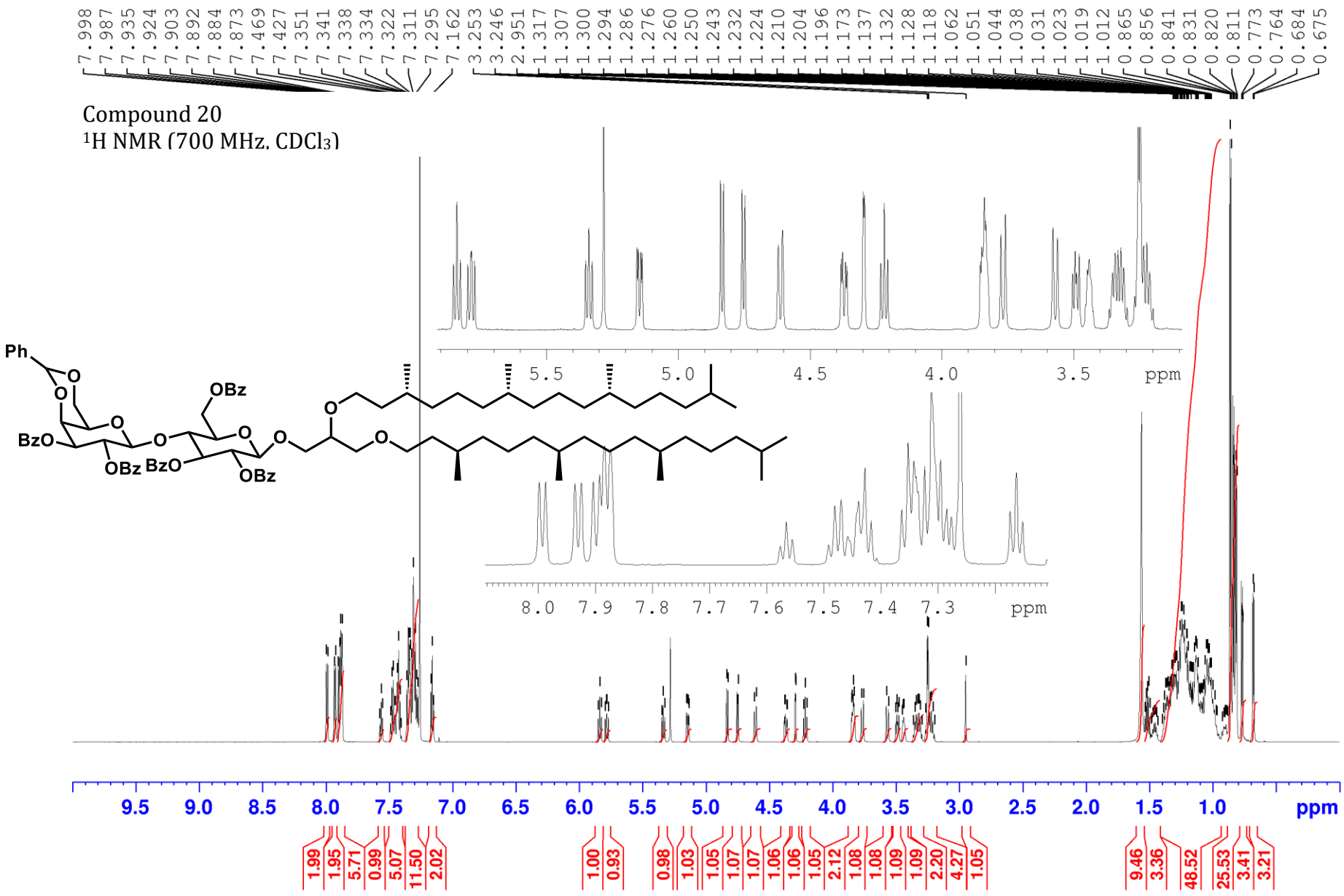
7.998
7.987
7.935
7.924
7.903
7.892
7.884
7.873
7.469
7.427
7.351
7.341
7.338
7.334
7.322
7.311
7.295
7.162
3.253
3.246
2.951
1.317
1.307
1.300
1.294
1.286
1.276
1.260
1.250
1.243
1.232
1.224
1.210
1.204
1.196
1.173
1.137
1.132
1.128
1.118
1.062
1.051
1.044
1.038
1.031
1.023
1.019
1.012
0.865
0.856
0.841
0.831
0.820
0.811
0.773
0.764
0.684
0.675
Compound 20
1H NMR (700 MHz, CDCl3)
Ph
OBz
BzO
OBz
BzO
OBz
5.5
5.0
4.5
4.0
3.5
ppm
8.0
7.9
7.8
7.7
7.6
7.5
7.4
7.3
ppm
9.5
9.0
8.5
8.0
7.5
7.0
6.5
6.0
5.5
5.0
4.5
4.0
3.5
3.0
2.5
2.0
1.5
1.0
ppm
1.99
1.95
5.71
0.99
5.07
11.50
2.02
1.00
0.93
0.98
1.03
1.05
1.07
1.07
1.06
1.06
1.05
2.12
1.08
1.08
1.09
1.09
2.20
4.27
1.05
9.46
3.36
48.52
25.53
3.41
3.21

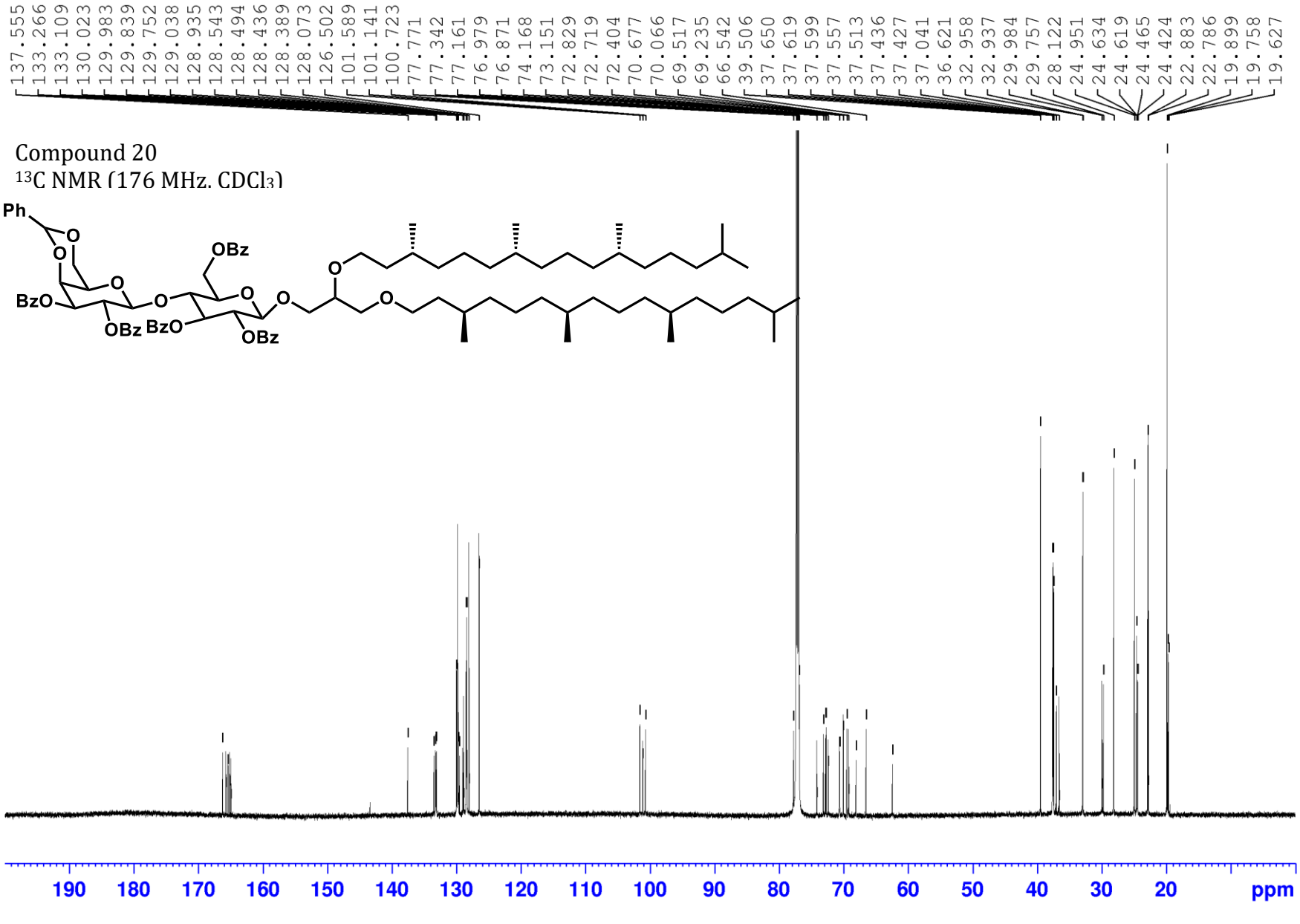
137.555
133.266
133.109
130.023
129.983
129.839
129.752
129.038
128.935
128.543
128.494
128.436
128.389
128.073
126.502
101.589
101.141
100.723
77.771
77.342
77.161
76.979
76.871
74.168
73.151
72.829
72.719
72.404
70.677
70.066
69.517
69.235
66.542
39.506
37.650
37.619
37.599
37.557
37.513
37.436
37.427
37.041
36.621
32.958
32.937
29.984
29.757
28.122
24.951
24.634
24.619
24.465
24.424
22.883
22.786
19.899
19.758
19.627
Compound 20
13C NMR (176 MHz, CDCl3)
Ph
OBz
BzO
OBz
BzO
OBz
190
180
170
160
150
140
130
120
110
100
90
80
70
60
50
40
30
20
ppm

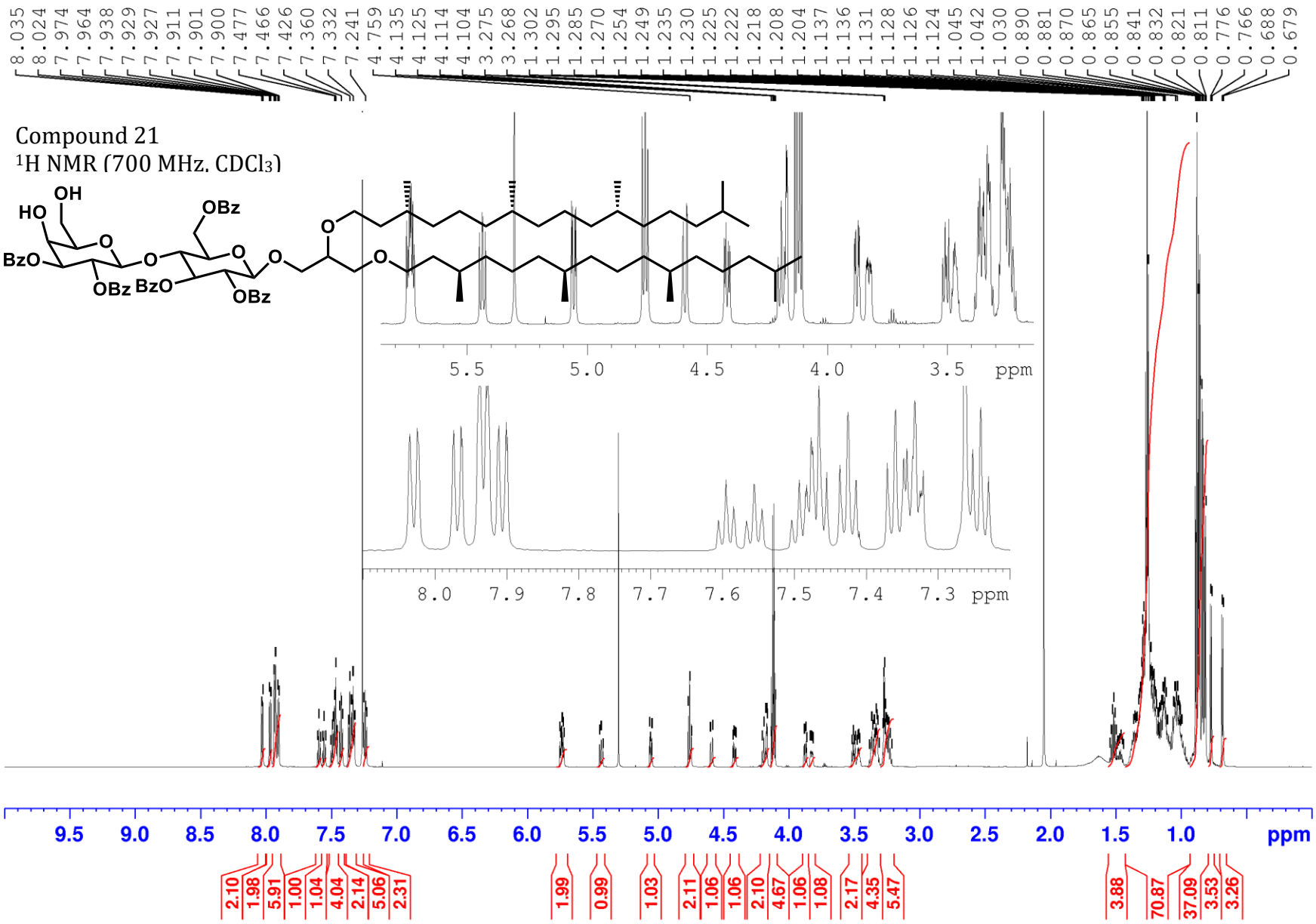
8.035
8.024
7.974
7.964
7.938
7.929
7.927
7.911
7.901
7.900
7.477
7.466
7.426
7.360
7.332
7.241
4.759
4.135
4.125
4.114
4.104
3.275
3.268
1.302
1.295
1.285
1.270
1.254
1.249
1.235
1.230
1.225
1.222
1.218
1.208
1.204
1.137
1.136
1.131
1.128
1.126
1.124
1.045
1.042
1.030
0.890
0.881
0.870
0.865
0.855
0.841
0.832
0.821
0.811
0.776
0.766
0.688
0.679
Compound 21
1H NMR (700 MHz, CDCl3)
OH
HO
OBz
BzO
OBz
BzO
OBz
5.5
5.0
4.5
4.0
3.5
ppm
8.0
7.9
7.8
7.7
7.6
7.5
7.4
7.3
ppm
9.5
9.0
8.5
8.0
7.5
7.0
6.5
6.0
5.5
5.0
4.5
4.0
3.5
3.0
2.5
2.0
1.5
1.0
ppm
2.10
1.98
5.91
1.00
1.04
4.04
2.14
5.06
2.31
1.99
0.99
1.03
2.11
1.06
1.06
2.10
4.67
1.06
1.08
2.17
4.35
5.47
3.88
70.87
37.09
3.53
3.26

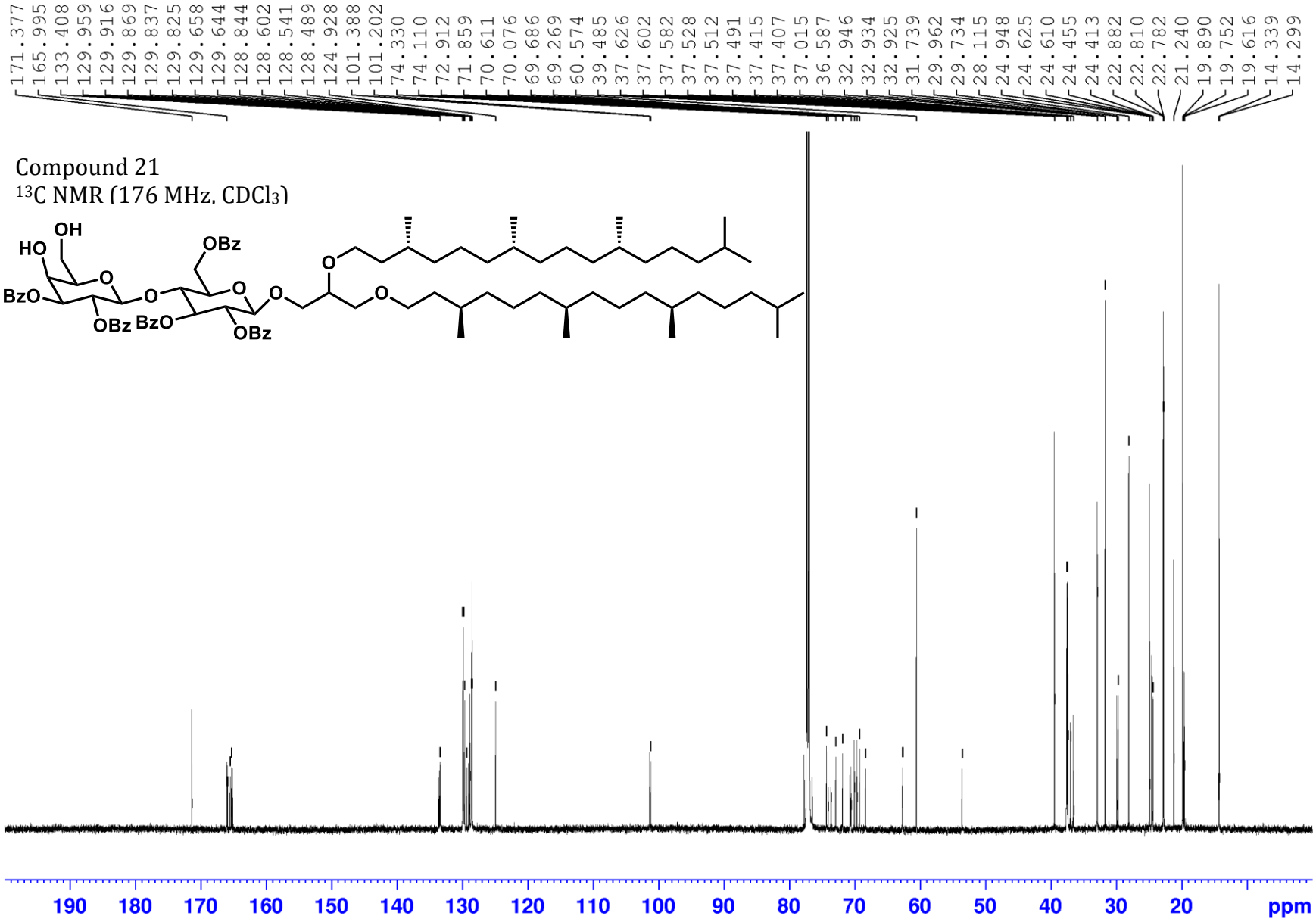
171.377
165.995
133.408
129.959
129.916
129.869
129.837
129.825
129.658
129.644
128.844
128.602
128.541
128.489
124.928
101.388
101.202
74.330
74.110
72.912
71.859
70.611
70.076
69.686
69.269
60.574
39.485
37.626
37.602
37.582
37.528
37.512
37.491
37.415
37.407
37.015
36.587
32.946
32.934
32.925
31.739
29.962
29.734
28.115
24.948
24.625
24.610
24.455
24.413
22.882
22.810
22.782
21.240
19.890
19.752
19.616
14.339
14.299
Compound 21
13C NMR (176 MHz, CDCl3)
OH
HO
OBz
BzO
OBz
BzO
OBz
O
190
180
170
160
150
140
130
120
110
100
90
80
70
60
50
40
30
20
ppm

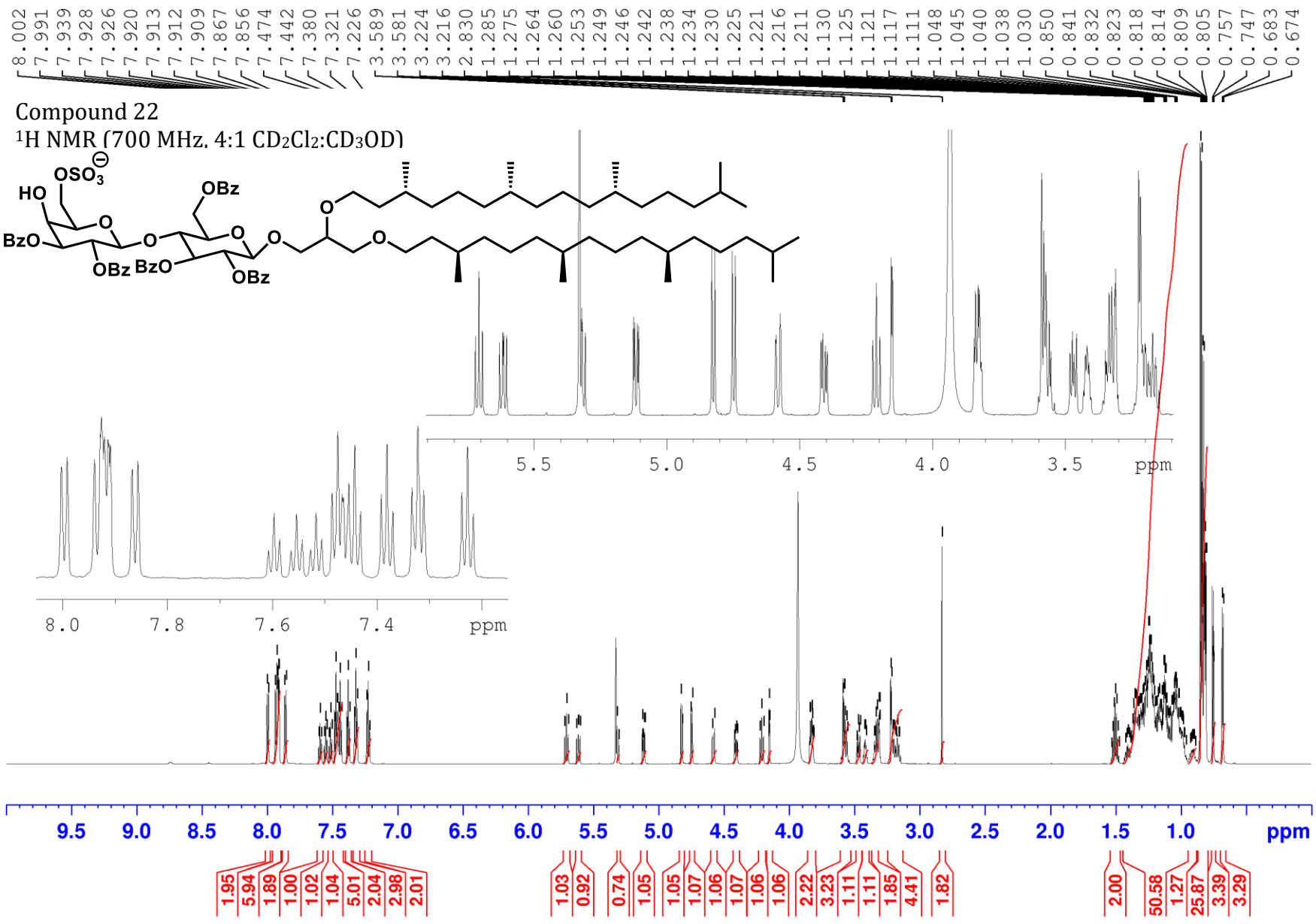
8.002
7.991
7.939
7.928
7.926
7.920
7.913
7.912
7.909
7.867
7.856
7.474
7.442
7.380
7.321
7.226
3.589
3.581
3.224
3.216
2.830
1.285
1.275
1.264
1.260
1.253
1.249
1.246
1.242
1.238
1.234
1.230
1.225
1.221
1.216
1.211
1.130
1.125
1.121
1.117
1.111
1.048
1.045
1.040
1.038
1.030
0.850
0.841
0.832
0.823
0.818
0.814
0.809
0.805
0.757
0.747
0.683
0.674
Compound 22
1H NMR (700 MHz, 4:1 CD2Cl2:CD3OD)
OSO3
HO
OBz
BzO
OBz
BzO
OBz
5.5
5.0
4.5
4.0
3.5
ppm
8.0
7.8
7.6
7.4
ppm
9.5
9.0
8.5
8.0
7.5
7.0
6.5
6.0
5.5
5.0
4.5
4.0
3.5
3.0
2.5
2.0
1.5
1.0
ppm
1.95
5.94
1.89
1.00
1.02
1.04
5.01
2.04
2.98
2.01
1.03
0.92
0.74
1.05
1.05
1.07
1.06
1.07
1.06
1.06
2.22
3.23
1.11
1.11
1.85
4.41
1.82
2.00
50.58
1.27
25.87
3.39
3.29

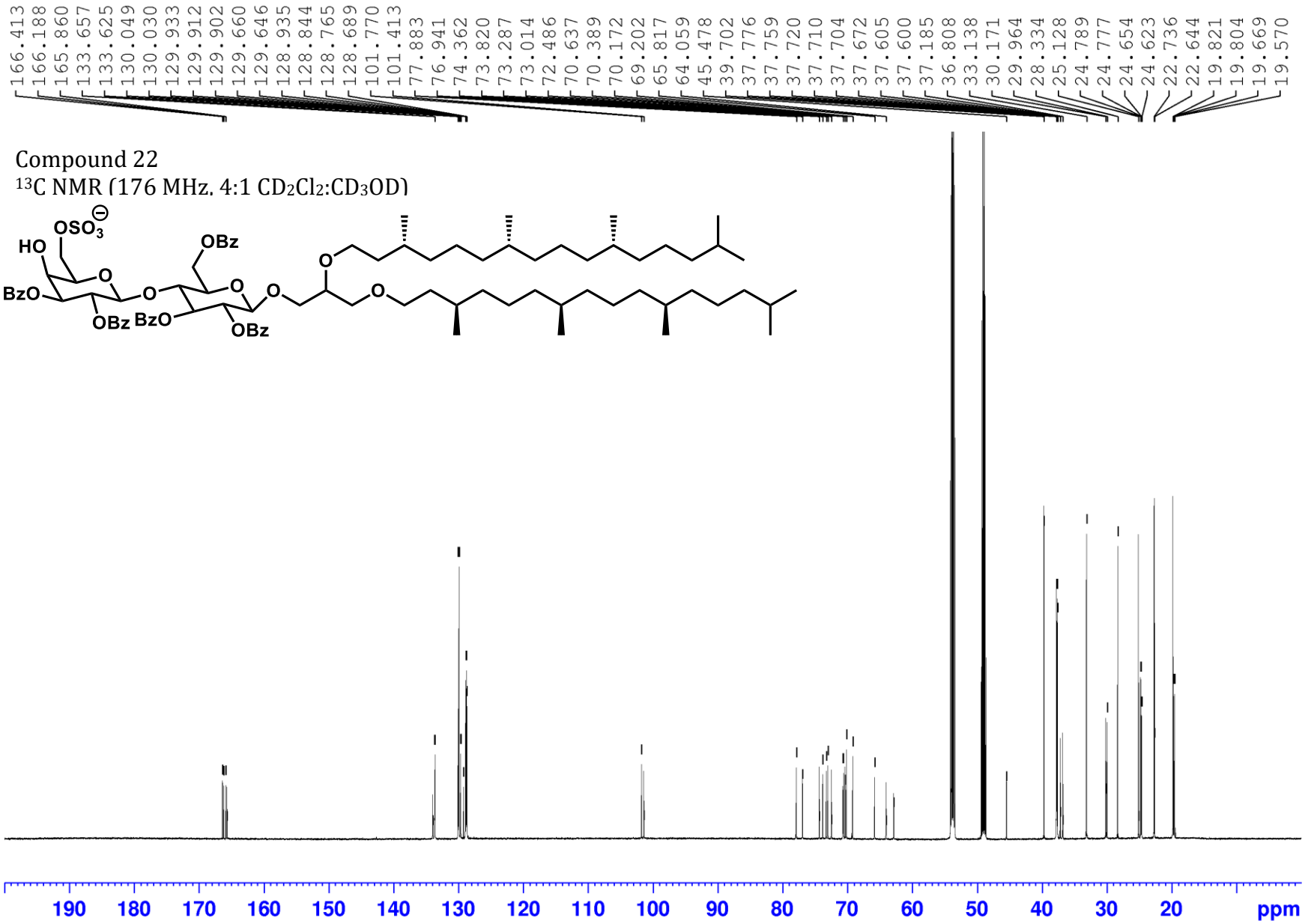
166.413
166.188
165.860
133.657
133.625
130.049
130.030
129.933
129.912
129.902
129.660
129.646
128.935
128.844
128.765
128.689
101.770
101.413
77.883
76.941
74.362
73.820
73.287
73.014
72.486
70.637
70.389
70.172
69.202
65.817
64.059
45.478
39.702
37.776
37.759
37.720
37.710
37.704
37.672
37.605
37.600
37.185
36.808
33.138
30.171
29.964
28.334
25.128
24.789
24.777
24.654
24.623
22.736
22.644
19.821
19.804
19.669
19.570
Compound 22
13C NMR (176 MHz, 4:1 CD2Cl2:CD3OD)
OSO3
HO
OBz
BzO
OBz
BzO
OBz
190
180
170
160
150
140
130
120
110
100
90
80
70
60
50
40
30
20
ppm

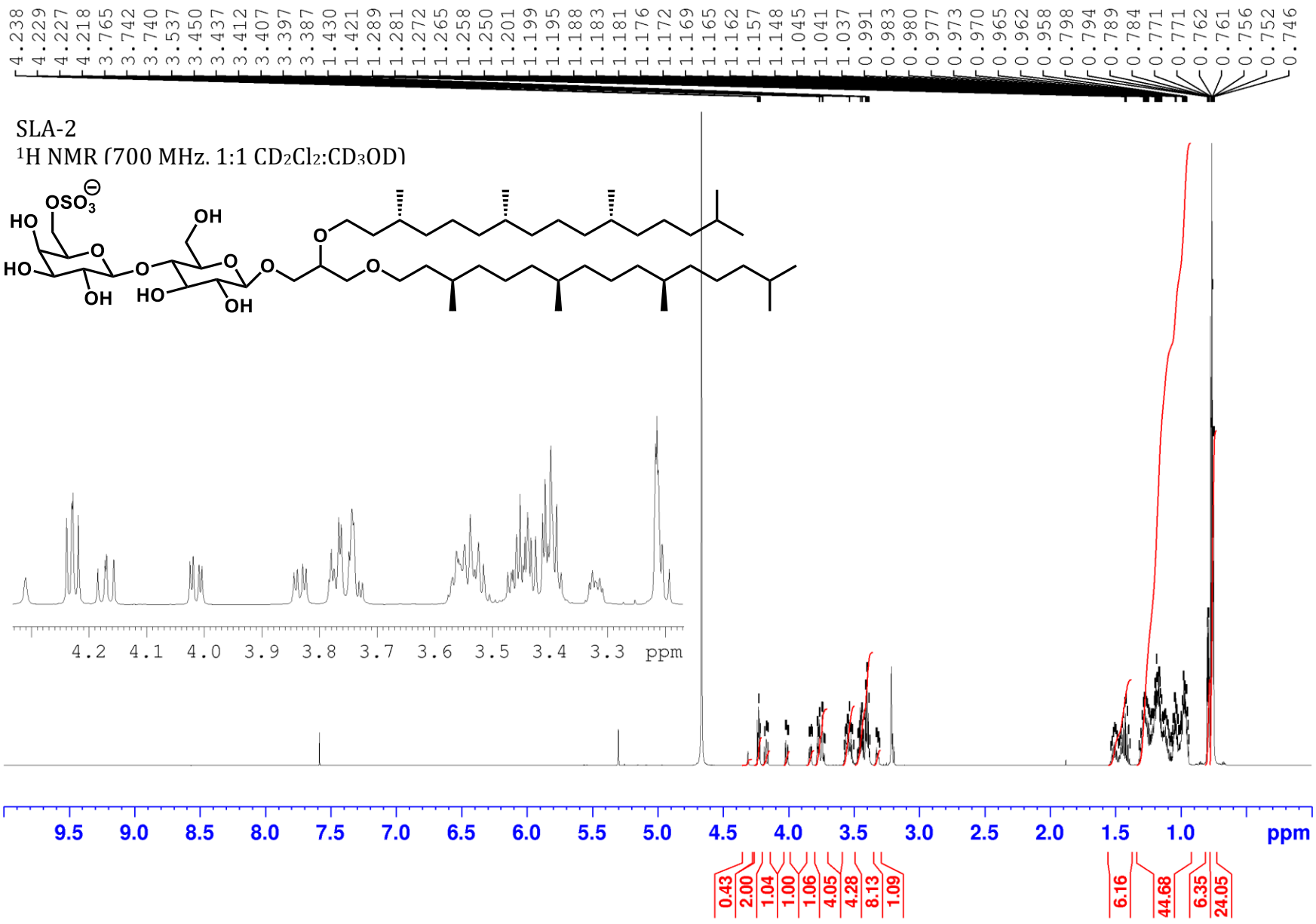
4.238 4.229 4.227 4.218 3.765 3.742 3.740 3.537 3.450 3.437 3.412 3.407 3.397 3.387 1.430 1.421 1.289 1.281 1.272 1.265 1.258 1.250 1.201 1.199 1.195 1.188 1.183 1.181 1.176 1.172 1.169 1.165 1.162 1.157 1.148 1.045 1.041 1.037 0.991 0.983 0.980 0.977 0.973 0.970 0.965 0.962 0.958 0.798 0.794 0.789 0.784 0.771 0.771 0.762 0.761 0.756 0.752 0.746
SLA-2
1H NMR (700 MHz, 1:1 CD2Cl2:CD3OD)
HO
OSO3
OH
HO
O
O
HO
OH
O
O
HO
OH
O
O
4.2 4.1 4.0 3.9 3.8 3.7 3.6 3.5 3.4 3.3 ppm
9.5 9.0 8.5 8.0 7.5 7.0 6.5 6.0 5.5 5.0 4.5 4.0 3.5 3.0 2.5 2.0 1.5 1.0 ppm
0.43 2.00 1.04 1.00 1.06 4.05 4.28 8.13 1.09
6.16 44.68 6.35 24.05

SLA-2

^{13}C NMR (176 MHz, 1:1

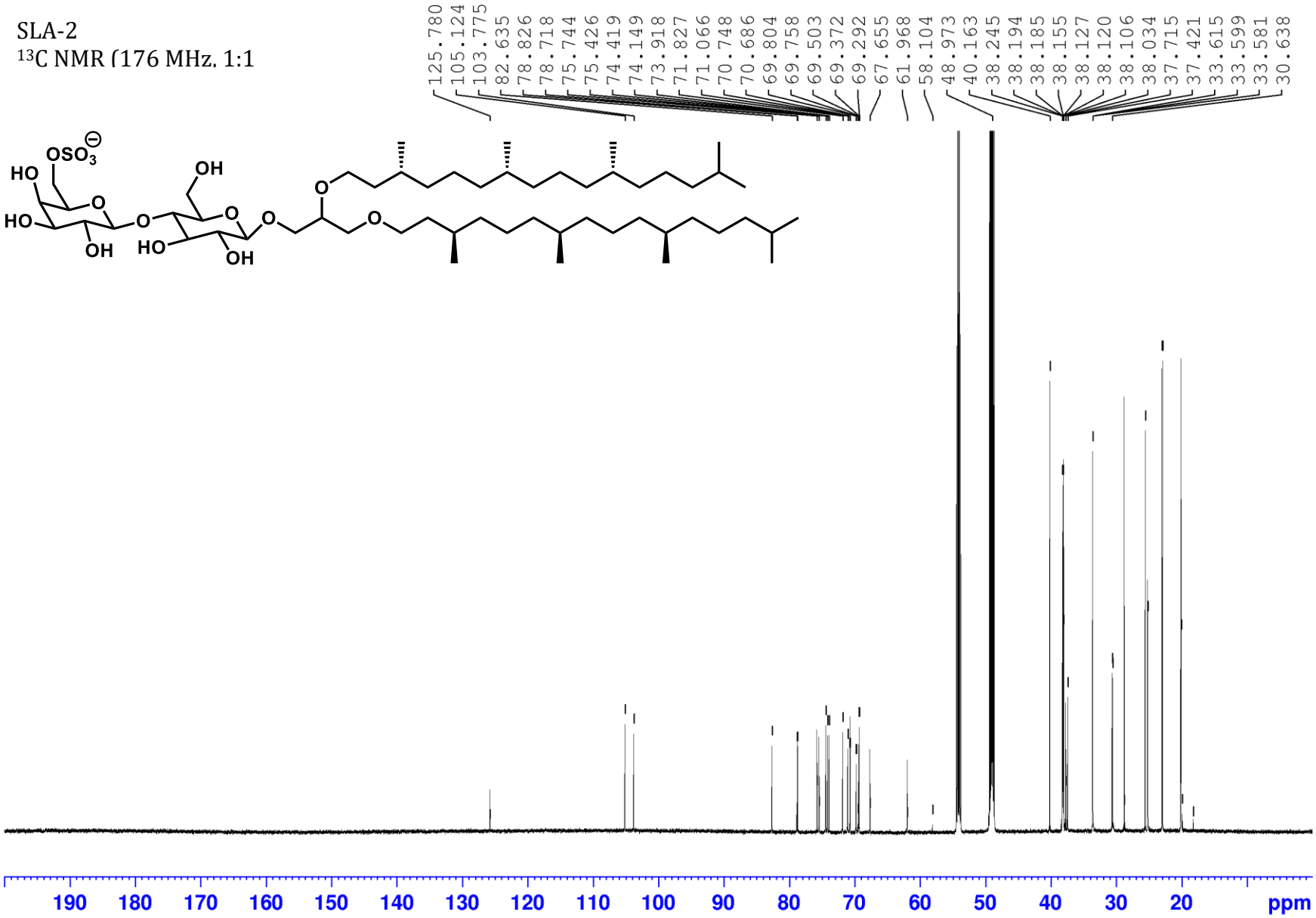

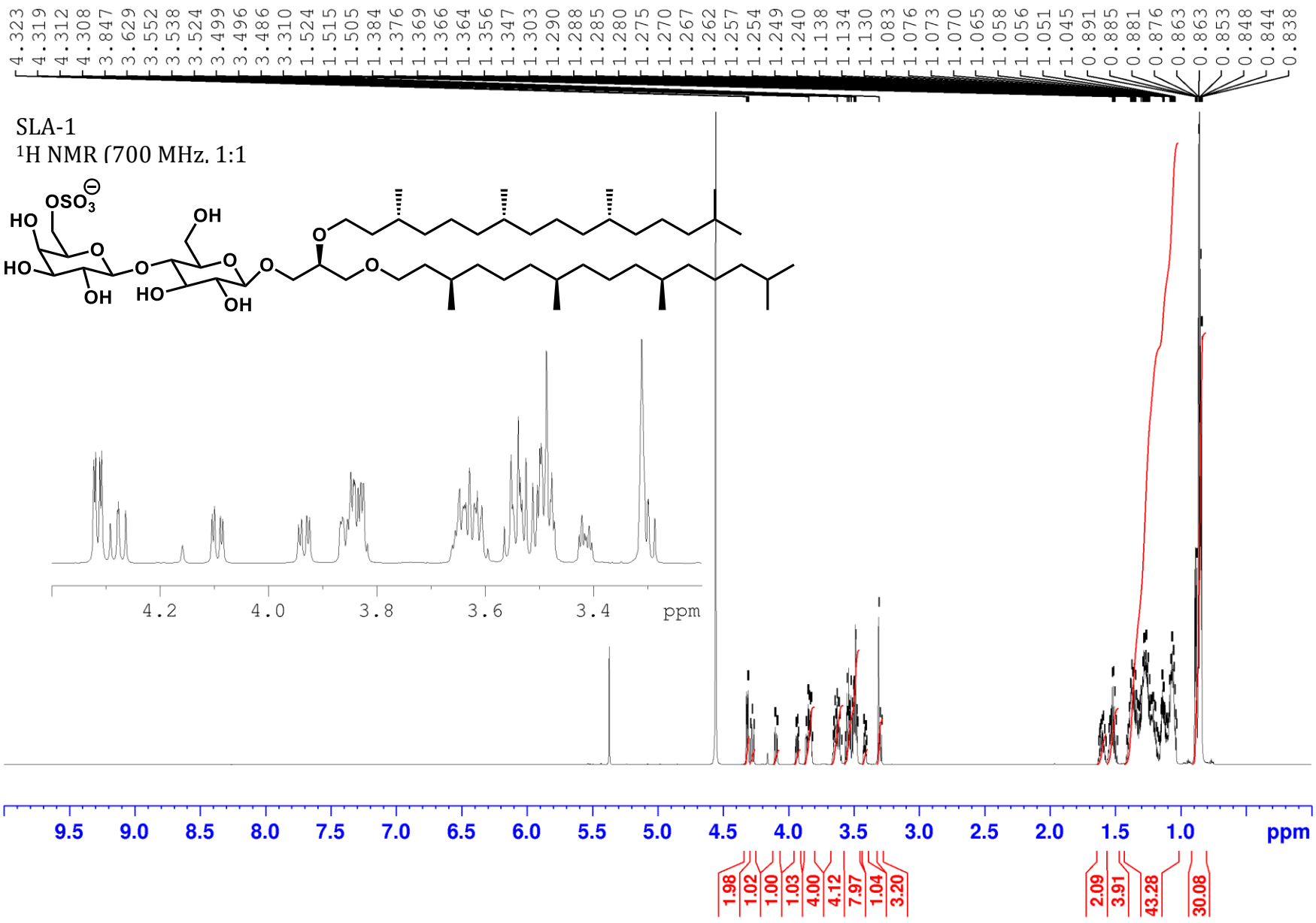
4.323 4.319 4.312 4.308 3.847 3.629 3.552 3.538 3.524 3.499 3.496 3.486 3.310 1.524 1.515 1.505 1.384 1.376 1.369 1.366 1.364 1.356 1.347 1.303 1.290 1.288 1.285 1.280 1.275 1.270 1.267 1.262 1.257 1.254 1.249 1.240 1.138 1.134 1.130 1.083 1.076 1.073 1.070 1.065 1.058 1.056 1.051 1.045 0.891 0.885 0.881 0.876 0.863 0.863 0.853 0.848 0.844 0.838
SLA-1
1H NMR (700 MHz, 1:1
HO
OSO3
OH
HO
O
O
O
O
HO
OH
OH
O
O
4.2
4.0
3.8
3.6
3.4
ppm
9.5 9.0 8.5 8.0 7.5 7.0 6.5 6.0 5.5 5.0 4.5 4.0 3.5 3.0 2.5 2.0 1.5 1.0 ppm
1.98 1.02 1.00 1.03 4.00 4.12 7.97 1.04 3.20
2.09 3.91 43.28 30.08

SLA-1

^{13}C NMR (176 MHz, 1:1

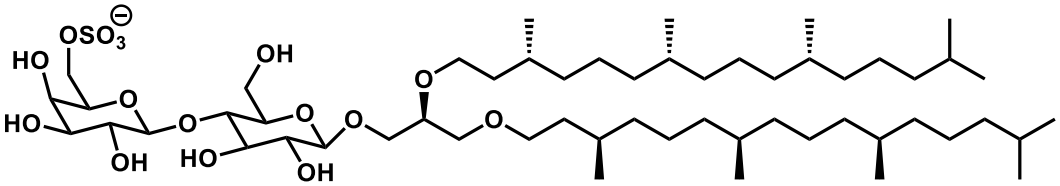

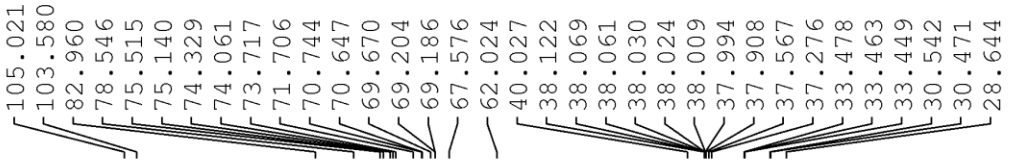

References

1. Whitfield, D. M.; Yu, S. H.; Dicaire, C. J.; Sprott, G. D., Development of New Glycosylation Methodologies for the Synthesis of Archaeal-Derived Glycolipid Adjuvants. *Carbohydrate Research* **2010,** *345* (2), 214-229.
2. Whitfield, D. M. S., G. D.; Krishnan, L. Sulfated-Glycolipids as Adjuvants for Vaccines. **2016**.
3. Prabha, S. P.; Karthik, C.; Chandrika, S. H., Phytol – a Biosurfactant from the Aquatic Weed Hydrilla Verticillata. *Biocatalysis and Agricultural Biotechnology* **2019,** *17*, 736-742.
4. Thakor, P.; Mehta, J.B.; Patel, R. R.; Patel, D. D.; Subramaniana, R. B.; Thakkar, V.R., Extraction and purification of phytol from Abutilon indicum: cytotoxic and apoptotic activity. *Royal Society of Chemistry Advances* **2016** (6) 48336–48345.